Methyl Radical Loss from Selected $C_6H_{10}O$ Isomers

Mehrshid Alai

A Thesis

in

The Department

of

Chemistry

Presented in Partial Fulfillment of the Requirements
for the Degree of Master of Science at
Concordia University
Montréal, Québec, Canada

December 1984

ABSTRACT

Methyl Radical Loss from Selected $C_6H_{10}O$ Isomers

Mehrshid Alai

The loss of methyl radical from the molecular ions of cyclohexenoxide, 5,6-dihydro-4-methyl-2H-pyran, mesityl oxide and methyl-1-methyl-cyclopropyl ketone has been investigated. On the basis of metastable peak shape analysis, CID/MIKE spectra and thermochemical data, it is concluded that the same $[C_5H_7O]^+$ ion is formed in the case of cyclohexenoxide and 5,6-dihydro-4-methyl-2H-pyran. Loss of CO from $[C_5H_7O]^+$ daughter ions of mesityl oxide and methyl-1-methyl-cyclopropyl ketone generates isomeric methyl-allyl ions.

TABLE OF CONTENTS

LIST OF FIGURES

LIST OF TABLES

I.A.OBJECTIVE

The objective of this work is to determine the site of methyl radical elimination from the molecular ions of selected $C_6H_{10}O$ isomers and to elucidate the structure of daughter ions generated. The subsequent fragmentation of daughter ion, $[C_5H_7O]^+$, also provides evidence for the existence of a common ion structure. Thermochemical data concerning the molecular ion, $[C_6H_{10}O]^{+\cdot}$, and the daughter ion, $[C_5H_7O]^+$, is reported. Metastable peak shape analysis of processes [m/z 98 to m/z 83] and [m/z 83 to m/z 55] as well as the collision induced dissociation spectra of the ions generated are the basis of the discussion.

I.B.INTRODUCTION

Preliminary studies on a number of $C_6H_{10}O$ isomers suggested significant similarities in the fragmentation pathways of these different precursors. Attention was

focused on the methyl radical loss from the molecular ions of isomers with different functionalities. On the basis of results obtained, several groups of compounds were formed, each exhibiting a common characteristic. One particular group, group A: 5,6-dihydro-4-methyl-2H-pyran, 1, and cyclohexenoxide (1,2-epoxycyclohexane), 2, was distinguished from others for its non-composite and tremendous methyl radical loss process in the metastable time frame. Group B: mesityl oxide (4-methyl-3-pentene-2-one), 3, and methyl-1-methyl-cyclopropyl ketone, 4, had a characteristic loss at the m/z 83 to m/z 55 stage.

The following is a summary of the mass spectral studies performed by other researchers on the above mentioned compounds and the direction taken thereby in this work.

A)

A limited number of studies has been reported on the mass spectral behavior of Δ^3-dihydro pyrans. Vul'fson et al., (1), investigated the electron impact fragmentation of 5,6-dihydro-4-methyl-2H-pyran, 1, and a number of other substituted analogues. Fragmentation processes as well as daughter ion structures were postulated for a number of cases, but not for the loss of methyl radical (1). Lately, Galkin et al., (2), reported that methyl loss generates the most intense peak in the mass spectrum of 1 at both high

and low ionizing energies, i.e. 70 and 12 electron volts, respectively. These authors suggested that this fragmentation may involve the C(4) substituent (2). In order to assign a structure to the daughter ion generated, the site of methyl elimination had to be determined.

The methyl radical loss from cyclohexenoxide, 2, is also the source of the most intense peak in the mass spectrum at both 70 and 12 eV ionizing energies. Using ^2H labelled analogues, Strong et al., (3), proposed three major mechanisms for $[M^{+\cdot}-CH_3\cdot]$, resulting in generation of three daughter ions a, b and c, (3). Significant similarities in the methyl loss from 1 and 2 were observed during the course of this study, specially in the metastable time frame. Therefore, the possibility of a common $[C_5H_7O]^+$ daughter ion was examined.

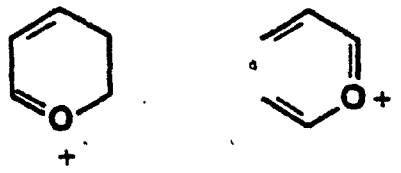

a

b

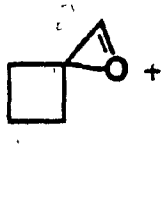

c

B)

Examining the kinetics of methyl elimination from ionized 2-methyl-1-penta-3,4-diene-2-ol, Zwinselman et al., (4), postulated the presence of the molecular ion of mesityl oxide, 3, as an intermediate structure and reported their results of specific ^{13}C and ^{2}H labelling. On the basis of their observations it was indicated that the methyl attached to the carbonyl group is involved in 90% of the methyl radical loss from the molecular ion of 3 (4).

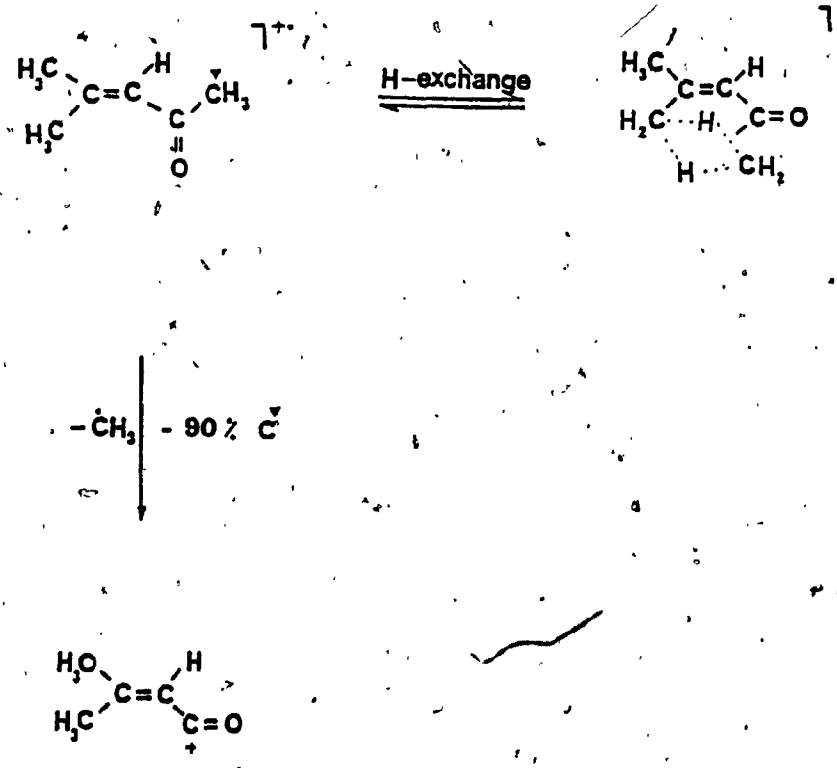

Scheme · I.1

During our studies, a distinct pattern was observed for the process of [m/z 83 to m/z 55] from both mesityl-oxide and methyl-1-methyl-cyclopropyl ketone, 4. For both compounds this process in the metastable time frame was associated with a significantly small magnitude of kinetic energy release. To understand the origin of this common character, the methyl radical loss from the molecular ions of 3 and 4 had to be looked into. No previous investigations has been reported on $[M^{+\cdot}-CH_3^{\cdot}]$ of methyl-1-methyl-cyclopropyl ketone; however, mass spectral behavior of a number of cyclopropyl derivatives has been the topic of various publications. Specifically, the fate of the cyclopropyl ring has attracted a great deal of attention. Experiments on a number of monosubstituted cyclopropyl derivatives suggest that the cation radical of cyclopropyl undergoes ring opening and hydrogen transfer prior to dissociation (5, 6). Schwarz et al., (7), in studying the isomerization patterns of substituted cycloalkanes reported that regardless of the nature of the substituent, ring opening exclusively involves the C_1 and C_2 bond, and a linear alkene radical cation is generated. The following is their proposed scheme for cyclopropyl derivatives (7).

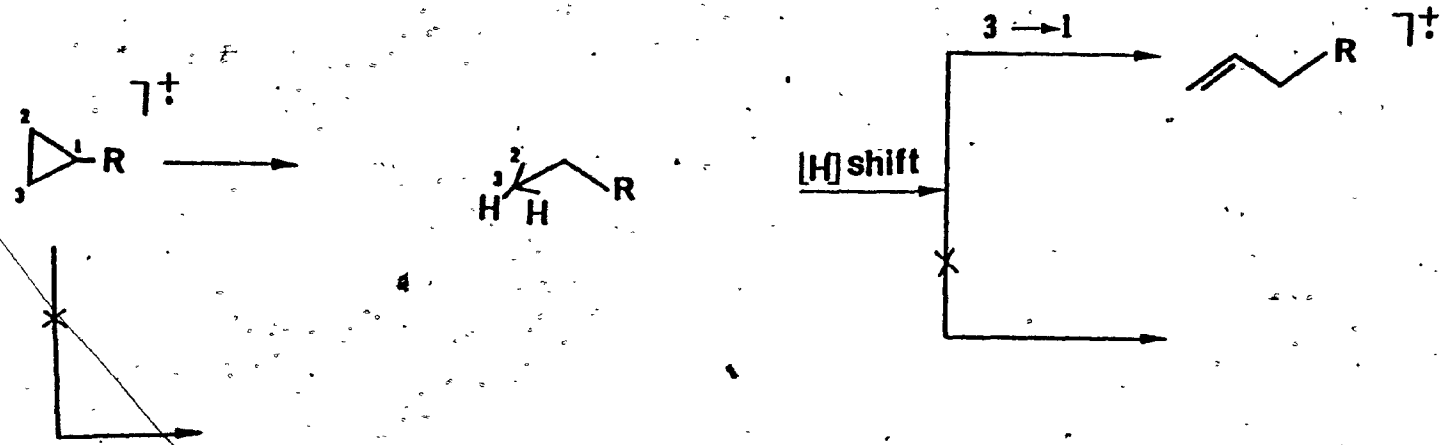

Scheme 1.2

II.THEORY

Organic mass spectrometry is concerned with the elucidation of reaction mechanisms, energetics and ion structures in the gas phase. When a beam of ions undergoes unimolecular fragmentation, depending on the type and the age of ion, a wealth of information with regards to the chemistry of organic ions is obtained.

A. The Mass Spectrometer:

Recent advances in mass spectrometry have resulted in a variety of sophisticated and powerful instruments. However, this introduction will be limited to a commonly used (in this work as well as elsewhere) double focusing mass spectrometer, the VG-micromass, type ZAB-2F which consists of (Fig.1):

1) an inlet system
2) an ion source and an accelerating field
3) the first field free region
4) a magnetic sector
5) the second field free region
6) an electrostatic sector (ESA)
7) an ion collector
8) an amplifier and a recording device

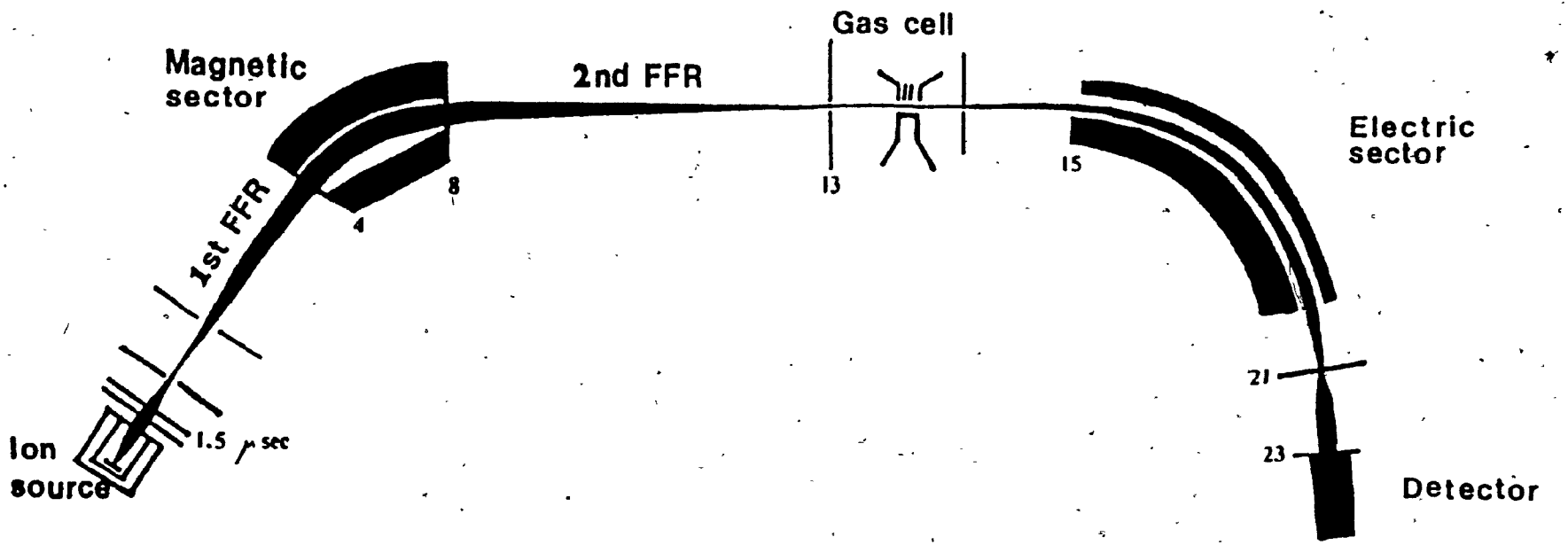

Fig.1, Ion optical system of the VG-Micromass spectrometer, type ZAB-2F.

In addition, a powerful vacuum system is required (8). Such an arrangement is often refered to as reversed geometry, since the magnetic sector preceeds the electrostatic analyser. One advantage of such geometry is the ability to perform energy analysis on mass selected ions (9). Numbers on the lower part of Fig.1 represent approximate time scale of events (in μsec) for an ion of m/z 100 in the accelerating field of 8000 volts.

i) The ion source and the acceleration region

In a typical EI source, under the impact of a beam of electrons produced from a heated filament, the gaseous molecules of the sample lose an electron, and positively charged molecular ions are generated. Further fragmentation of such ions results in a number of daughter ions:

$$M + e \longrightarrow M_1^{+\cdot} + 2e$$

$$M_1^{+\cdot} \longrightarrow M_2^{+} + M_3^{\cdot}$$

$$\searrow M_2^{+\cdot} + M_3$$

With the aid of a repeller electrode bearing a small positive potential, ions formed are directed towards

the exit slit of the source. These ions have only a small range of potential energy in addition to their thermal energy spread. Upon arriving to the acceleration region they fall through a potential difference of several kVs, e.g. 8kV, acquire translational energy and go through the flight path. The main ion beam is hence the one having a kinetic energy equal to the full accelerating energy (10).

ii) The magnetic analyzer

For ions of charge ze and velocity v subjected to a magnetic field B perpendicular to their trajectory, the following condition must be satisfied:

$$Bze = Mv/R \qquad (1)$$

where M is the mass of the ion and R is the radius of the ion path curvature. The kinetic energy of the ion will be:

$$1/2\ Mv^2 = zeV \qquad (2)$$

hence:

$$M/ze = (R^2B^2/2V) \qquad (3)$$

From the above, it is clear that the magnetic analyzer is a momentum separator and the commonly used " m/z" is representative of the " mass-to-charge number ratio", where e is the unit charge. In the single focusing mode, scanning the magnetic sector will generate the conventional mass

spectrum, containing peaks due to the molecular ion and its fragment ions. In addition to ions being formed in the source, if any fragmentation takes place in the first field free region, the region between the ion acceleration and the magnetic sector, it will be detected as a small diffuse metastable peak with the apparent mass of m_2^2/m_1 (11). Such peaks may be hard to pick out as they are often partially or completely covered by a larger peak, and are very much less intense than the normal peaks in the spectrum.

iii) The electrostatic analyzer

For ions subjected to the action of a circular electrostatic field perpendicular to their trajectory, a circular path of radius r will be followed if:

$$zeE = Mv^2/r \qquad (4)$$

where E is the electrostatic field.

Following equations 2 and 4 :

$$r = 2V/E \qquad (5)$$

Hence, the electrostatic analyzer is a kinetic energy separator and fragmentation of mass selected ions within the second field free region, Fig.1, will be separated on the basis of their energy-to-charge. Scanning the electric sector voltage downward will result in an ion

kinetic energy spectrum, resulted from the unimolecular fragmentation of a mass selected ion, MIKE (mass analysed ion kinetic energy). Since the voltage scale between E, the electric sector voltage necessary to transmit the parent ion, and zero corresponds linearly to the mass scale of daughter ions, the following relationship exists:

$$E_1 / E_2 = m_1/m_2 \qquad (6)$$

This fragmentation may also be associated with a considerable amount of translational energy release, T, which will be discussed later, (12).

Lately, the use of collision gas to excite the ion beam and to induce fragmentation has become widespread. The gas cell is often placed in the second field free region, prior to the electrostatic analyzer. Upon collision of the neutral gas molecules with the ions passing through the cell a variety of high intensity fragmentations takes place. Daughter ions generated are charge-to-energy separated by scanning down the electric sector (11).

The analogy of the mass spectrometer as a complete chemical laboratory can now be witnessed. Synthesis of ions takes place in the source, the magnetic analyzer purifies the ions, in the collision cell reaction of pure ions takes place and the resulting ions are analyzed by the electric sector (11).

B) METHODS FOR ION STRUCTURE DETERMINATION

The following are the main experimental methods employed in the determination of ion structures and fragmentation mechanisms. Each of these techniques may also be used in conjunction with site specific isotope labelling:

-Ion Thermochemistry
-Metastable Ion Characteristics
-Collision Induced Dissociation Spectra

It is important to note that each technique samples ions of different life times and internal energies. Table 1 is a summary of these variations.

The information obtained from each method is also dependent on the isomerization barrier. If the isomerization barrier is much higher than the lowest threshold for decomposition, all methods yield the same information. If the isomerization barrier is lower than the lowest threshold for decomposition, the thermochemical data and the collision induced dissociation spectra will show the existence of two structures, whereas metastable ion characteristics will result in information on isomerized ions only (13).

Table 1, Life time and energy dependencies of techniques used in ion structure determination, (13).

Technique	Energy[a]	Lifetime	Characteristic
Ion Thermo-chemistry	0	∞	Ions in their electronic and vibrational ground state
Metastable Ion Characteristic	E	10^{-6} -10^{-5}	Decomposing ions with a narrow range of internal energies just above the threshold for decomposition, up to $\sim$ 1eV.
Collision Induced Dissociation	0-E_o	$>10^{-5}$	Non-decomposing ions with internal energies between 0 and E_o.

a) E_o = lowest threshold for decomposition.

i) Ion Thermochemistry

For the reaction

$$AB^{+\cdot} \longrightarrow A^{+} + B^{\cdot}$$

$$\Delta H_f\,(AB^{+\cdot}) = IE + \Delta H_f\,(AB)$$

the heat of formation of the molecular ion can be determined from the heat of formation of the neutral molecule and the adiabatic ionization energy, IE.

The heat of formation of the daughter ion can be estimated from the following:

$$\Delta H_f(A^{+}) = AE + \Delta H_f(AB) - \Delta H_f(B^{\cdot}) - E_{excess}$$

where AE is the energy required for the appearance of the daughter ion peak, and E_{excess} may partially be estimated from the magnitude of the kinetic energy release in the metastable time frame (14), Fig.2.

Since the heat of formation of each ion is characteristic of that particular structure, the same or different heats of formation may imply identical or different ion structures. The information obtained, as mentioned previously corresponds to the ionization threshold (in the case of the molecular ion) or the formation threshold (in the case daughter ion) structure which may or may not be the same as the ion structure(s) studied in other time and energy frames.

Another practical importance of gas phase ion thermo-

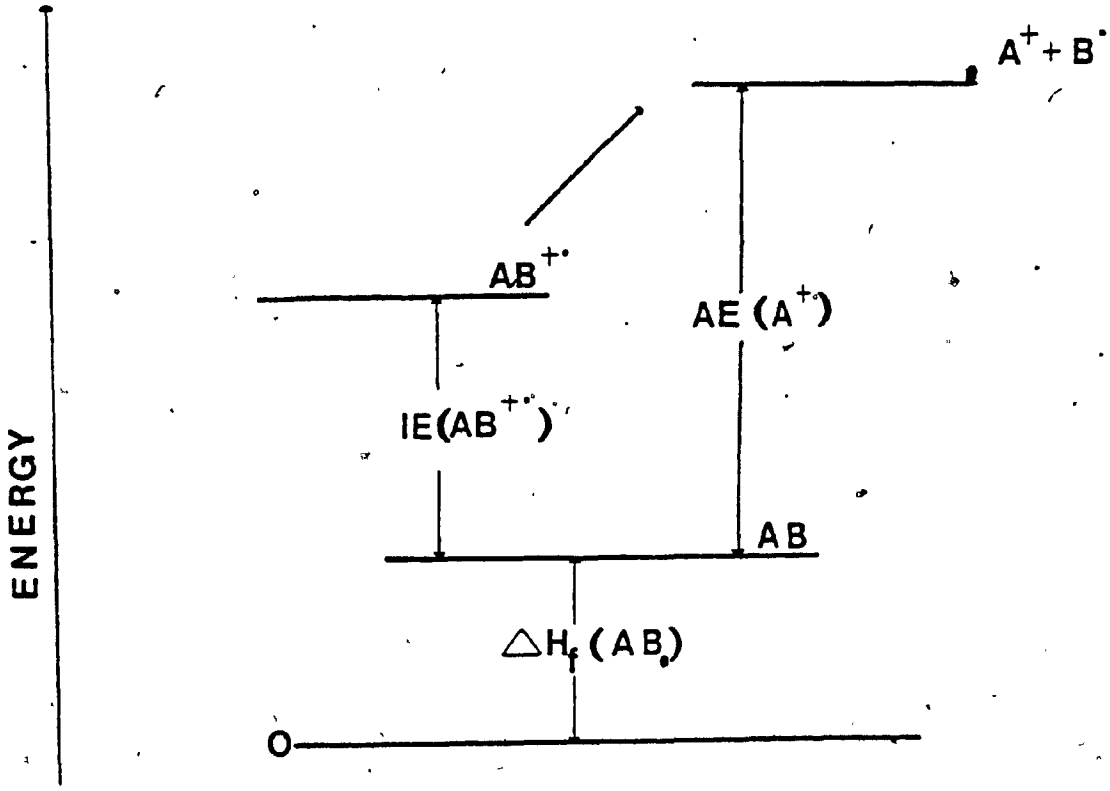

Fig.2. Energy diagram for generation and fragmentation of an ion $[AB]^{+\cdot}$

chemistry is in determination of the location and distribution of charge in ions of a homologous series. Heats of formation of organic ions can be estimated using relationships between the $\triangle H_f$ of ions differing only by the number of substituent group at or adjacent to a charge bearing atom. Recently, Holmes et al., (15), showed that the ionization energies of a homologous series are linear with relation to the reciprocal number of atoms, Fig.3, and expanded such meaurements to estimation of heat of formation of ions of

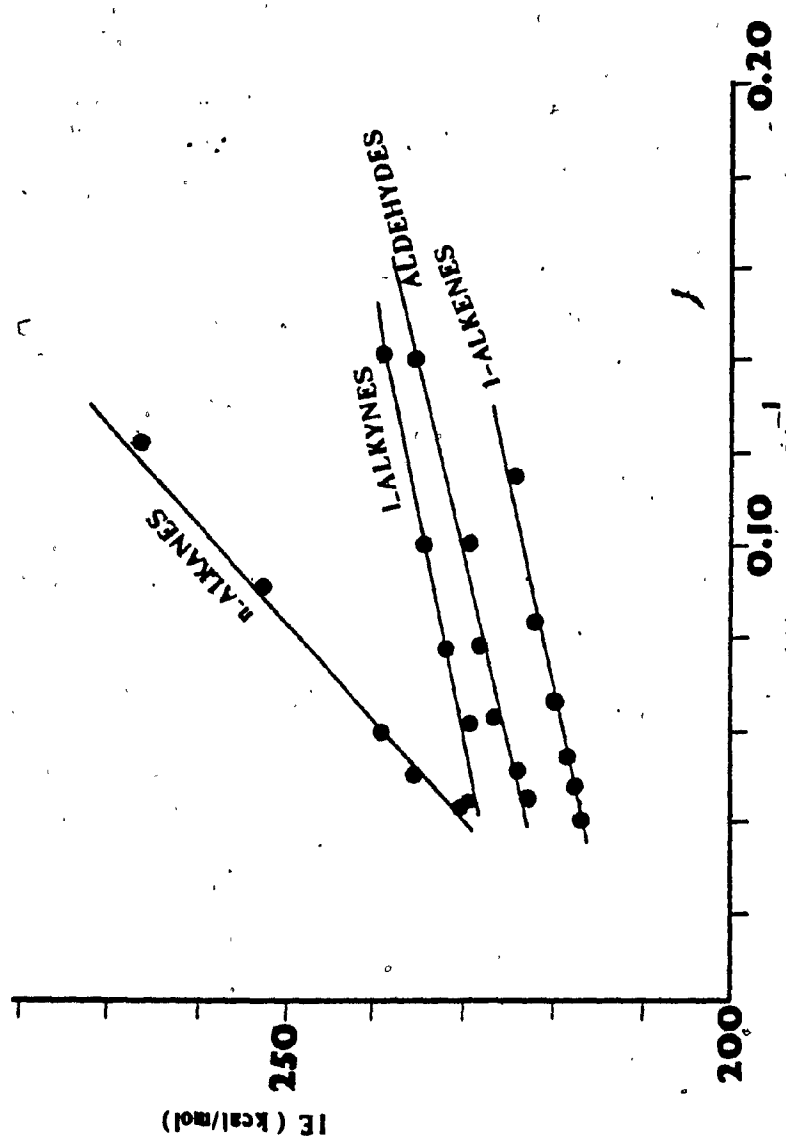

Fig.3. Ionization energies of linear-homologous molecules vs. (number of atoms)$^{-1}$.

interest.

In addition to difficulties with estimating excess energy, it should be realized that there are other problems associated with this technique. For example, different ions may coincidently have the same heat of formation. The use of conventional mass spectrometers in measuring IE values lowers the accuracy by 10-20 kJ/mol, and AE values are even less reliable (16).

ii) Metastable Ion Characteristics

Studying the relative abundances of daughter ions generated from a particular precursor in the metastable time frame and comparing their relative abundances with other isomeric ions could be important in assigning ion structures. Two identical ions of different origin will result in the same type of metastable fragments with similar abundance ratios. In the reverse geometry instrument, scanning the electric sector voltage will result in a MIKE (mass analysed ion kinetic energy) spectrum. Because of the sensitivity of MIKE spectrum to the internal energy distribution of fragmenting ions, no hypothesis can be established on the basis of MIKE spectra alone(17, 18).

By adjusting the instrumental conditions for best energy resolution, metastable peak shapes and the kinetic energy releases could be studied, which are less sensitive to energy distribution than MIKE spectra. The slow decomposition taking place in a field free region of the mass spectrometer is usually accompanied by the release of translational kinetic energy. This energy release determines the shape of the metastable peak observed.

For the fragmentation

$$AB^{+\cdot} \longrightarrow A^{+} + B^{\cdot}$$

the energy profile is:

$$AE(A^{+}) - IE(AB^{+\cdot}) = \Delta H_f(A^{+}) + \Delta H_f(B^{\cdot}) - \Delta H_f(AB^{+\cdot}) + E_{excess}$$

The excess energy determines the internal energy and the kinetic energy of the fragment ion, and itself is composed of two terms:

$$E_{excess} = E^{\neq} + E_r$$

$E^{\neq}$ designates the energy required to achieve rate constants appropriate to the observational time frame of the experiment. It also represents the non-fixed energy which is statistically partitioned between degrees of freedom. E_r is the difference between the enthalpies of the transition state and the final state. It is dependent on the reaction and inpendent of operational conditions, and is also referred to as fixed energy or the reverse activation energy. A fraction

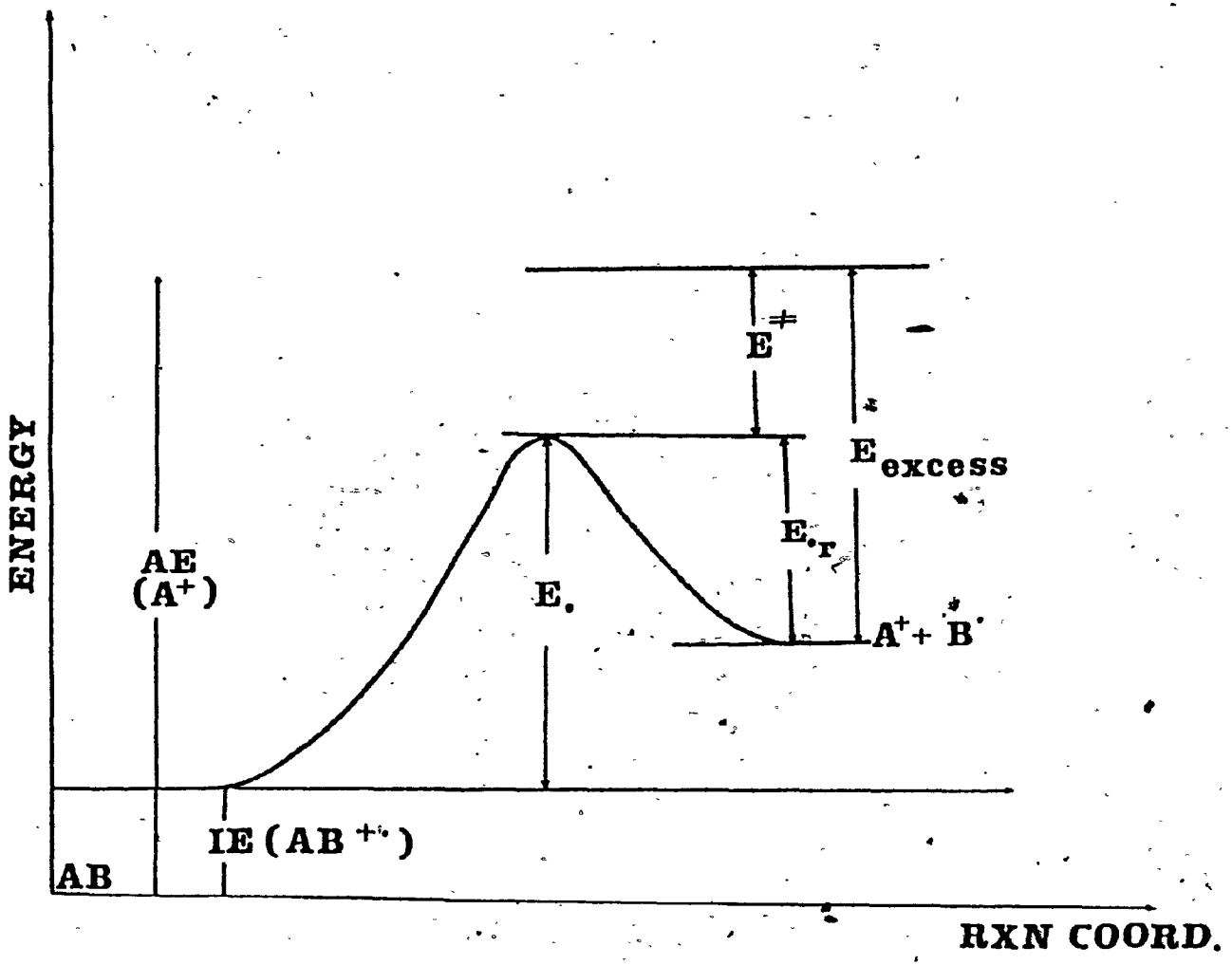

Fig. 4. Energy diagram for the process $AB^{+\cdot} \longrightarrow A^{+} + B^{\cdot}$ in the metastable time frame.

of E_{excess} gives rise to the term T, the amount of kinetic energy released. As a rule of thumb, if T is small it is representative of $E^{\neq}$ and $E_{.r}$ is negligible; if T is large $E_{.r}$ is the major contributor and involvement of $E^{\neq}$ is small. In the case of simple cleavage T is small and $E_{.r}$ is almost nil, e.g. the reaction of an ion with a radical does not require much activation energy; whereas, in the case of rearrangement reactions, the reverse activation energy is significant (14).

Gaussian-type metastable peaks are often observed with a small release of kinetic energy. The presence of such peaks is usually indicative of simple cleavage and a single reaction channel. A composite metastable, however, is representative of the number of reacting configurations involved and/or the number of daughter ions generated. They often contain a narrow component, (small T), superimposed on a broader one, (larger T), Fig.5. Reducing the ionizing energy may suppress one of the reaction channels (the component of higher AE), and change the peak shape. Isotope labelling has in many instances separated one component from the other(s), (17).

The width of the metastable peak at a selected height is a measure of the kinetic energy released upon fragmentation. This measured value is usually corrected for the energy spread of the main beam at the same height, assuming

Fig.5. Relative metastable peak shapes with respect to E_{excess} and T.

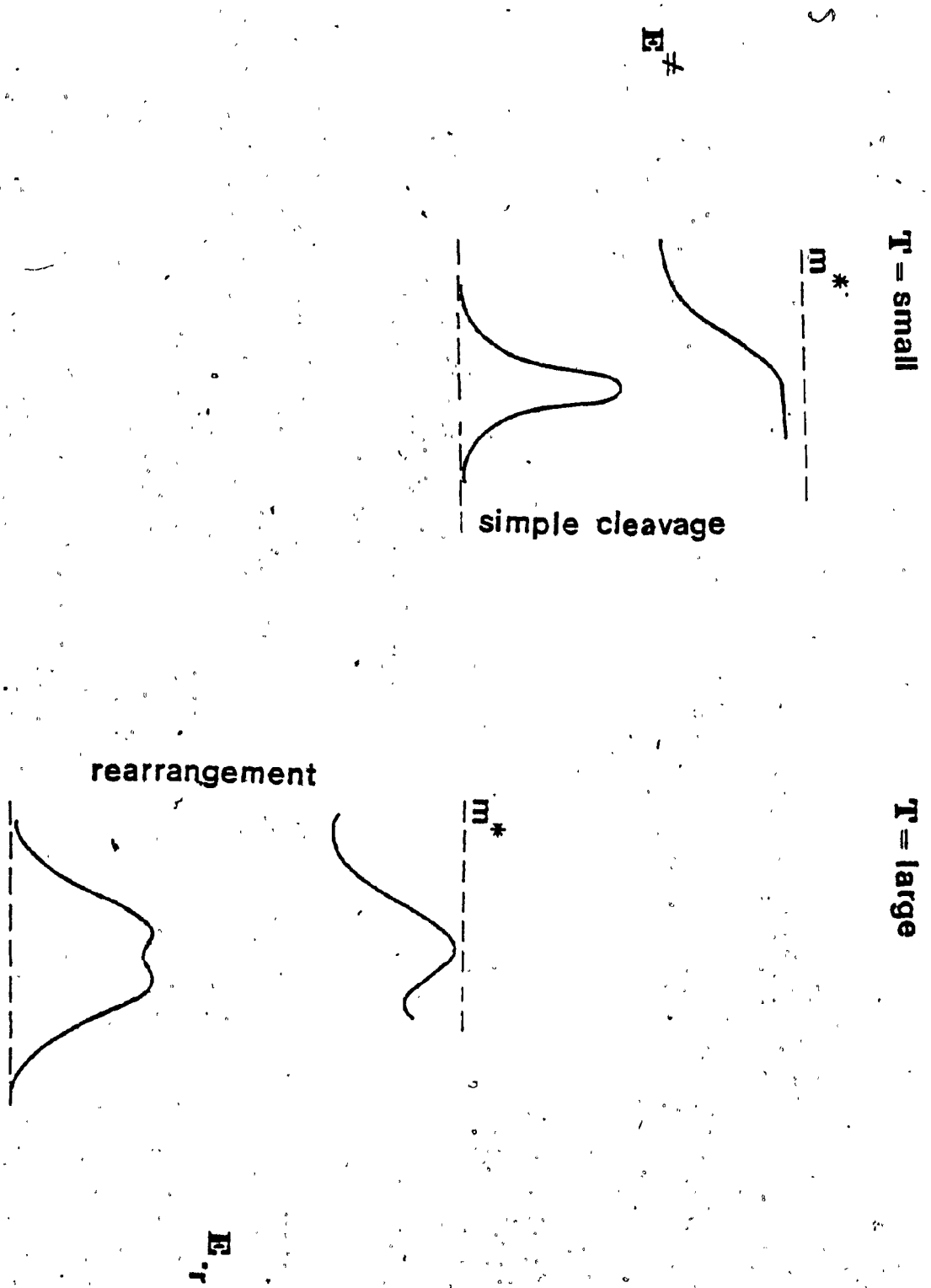

assuming that the main beam is much narrower than the metastable peak (16). Since T represents the amount of kinetic energy released from 'decomposing ions', its value has been used as a characteristic of the fragmentation process. If fragmentation of two isomeric ions gives rise to similar T values, identical reaction channels and/or daughter ions are assumed. Ions of the same structure but different precursors, in general, give rise to similar T values, (14). Additional and different experiments are required to verify such hypothesis. For example, ion aging, i.e. reducing the acceleration voltage may reveal the unexpected presence of two or more reaction channels, change the overall metastable peak shape and alter the $T_{0.5}$ values (19).

iii) Collision Induced Dissociation Spectra

When ions that do not have enough energy or the right configuration to fragment collide with atoms or molecules of a neutral gas, translational energy of the ion is converted into electronic excitation and a number of daughter ions are produced (20). For example, when helium is used as the collision gas, several electron volts are transfered and there is a significant increase (by a factor of hundred or more) in the number of ions fragmenting in the field free region collision cell (21).

Therefore, collision induced fragmentation involves two processes, Fig.6:

$$m_1^+ + N \longrightarrow m_1^{+*} + N$$ bimolecular excitation (endothermic)

$$m_1^{+*} \longrightarrow m_2^+ + m_3$$ unimolecular fragmentation (exothermic)

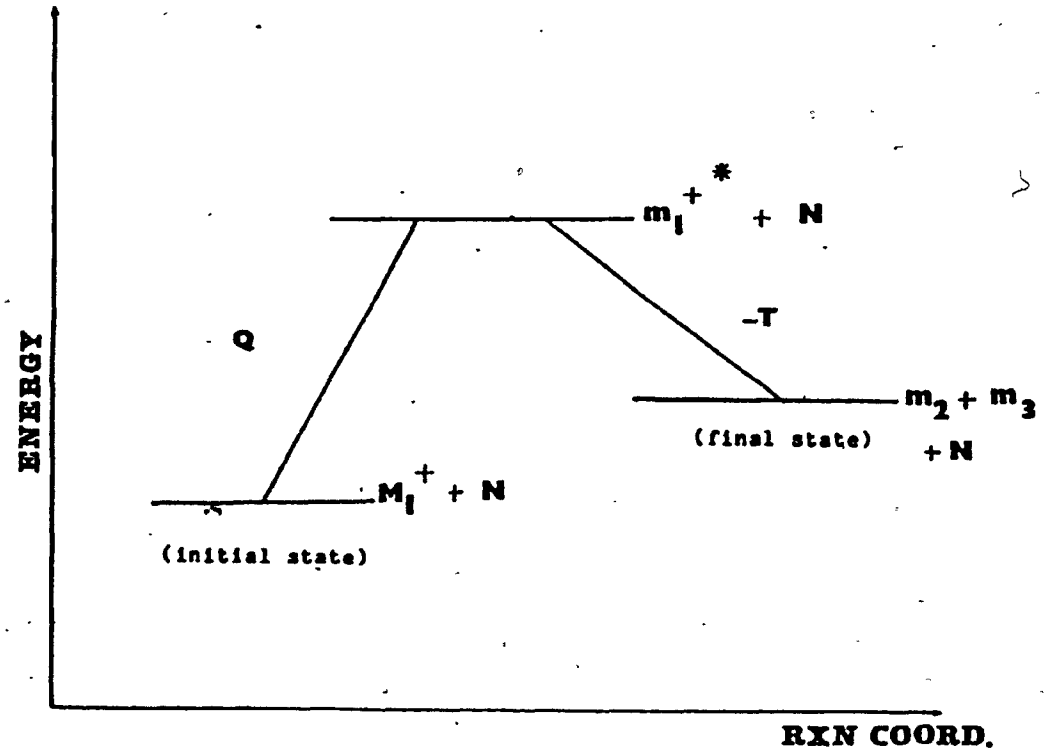

Fig.6. Energy diagram of a typical collision induced dissociation process.

Q= excitation energy
T= kinetic energy release

In terms of formation and decomposition the collision induced dissociation spectrum resembles the normal mass spectrum and hence could be indicative of the structure of the precursor ion (22).

Since metastable ion decompositions are detected in the same manner as the collision induced fragment ion peaks (only without the collision gas) there will be MI contributions in the CID spectrum, and often a correction for these processes is required.

It has been argued that the collision induced dissociation spectrum is independent of the precursor ion's internal energy, however, this point is still unresolved (23, 24). In order to avoid any confusion, it is suggested that ions of lower internal energies be selected for collision induced dissociation. For example, the CID spectrum of metastably generated daughter ions, or of ions produced at lower ionizing energies is less affected by internal energy variations (25).

Lately, the structure of the neutral products of ion fragmentations has been determined by collision induced dissociative ionization and observation of subsequent fragmentation. For example, application of this new technique distinguishes between HCN and HNC fragments from pyridine and aniline, respectively (26). Loss of CH_2OH rather than CH_3O from ionized methyl-acetate has been established by this method as well (27).

III. EXPERIMENTAL

A) COMPOUNDS

i) Origin:

The unlabelled compounds were purchased from the Aldrich Chemical Company, Milwaukee, and were used without further purification. Mass and NMR spectra of these compounds were comparable to the ones reported in the literature.

Labelled compounds were synthesised using labelled starting materials, bought from Merck Sharp and Dohme, Montreal. Because of the emphasis on mass spectral behavior rather than synthesis, yields were not optimised as long as sufficient amount of the desired product was obtained.

ii) Synthetic Procedures:

The 5,6-dihydro-4-CD_3-2H-pyran was prepared from 4-methoxy-5,6-dihydro-2H-pyran and CD_3-MgI by a procedure analogous to the synthesis of methyl cyclohexane from methoxy-cyclohexane (28). As the yield was low, the final product was taken up in xylene and redistilled. Collected fractions were analysed using gas chromatography and the fraction richest in the product of interest was used for gas chromatography- mass spectrometry. Analysis of the

reaction products indicated the presence of two isomers the desired isomer was obtained pure by preparative gas chromatography at 60° C using a 3% O.V.-17 column.

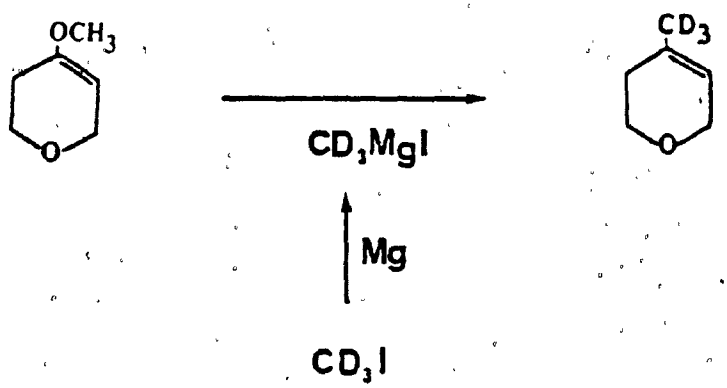

The CD_3,1-methyl-cyclopropyl ketone was prepared by a base catalysed exchange of methyl-1-methyl cyclopropyl ketone with D_2O, over a period of 48 hours. The reaction mixture was extracted with ether, and the ether extract was dried over $MgSO_4$ and concentrated. The final product was identified by GC, and the site of labelling was determined by NMR.

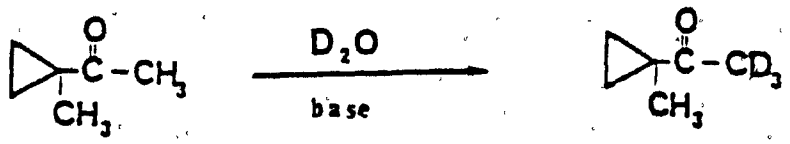

B) INSTRUMENTATION

i) Double Focusing Mass Spectrometer:

A Hitachi Perkin Elmer RMU-7 mass spectrometer of reversed geometry was used to perform preliminary studies. This instrument was equipped with a 0-500V ESA power supply driven by a 0-20V ramp generator. Sample pressure was approximately 3.5×10^{-6} mm Hg and the accelerating voltage was 2.5-3 kV.

Further experiments were performed on a VG-Micromass spectrometer, type ZAB-2F, of reversed geometry, fitted with a collision cell located immediately prior to the ESA enterance slit, Fig.1. The acceleration voltage was 8 kV, and sample pressure was about 4×10^{-7} mbar.

Ionization potential and appearance energies were measured by Dr.F.P.Lossing at the University of Ottawa, using monoenergetic electron impact as described elsewhere (29, 30).

Metastable appearance energy measurements, using the method suggested by Burgers et al, (31), were performed on a Kratos AEI MS-902S mass spectrometer at the University of Ottawa.

a) Conventional mass spectra: Samples were admitted to the electron impact source via a Granville-Phillips variable leak valve or a heated septum inlet at 150 C. Once the instrument was optimized for maximum signal intensity, the magnet was scanned and the spectrum was recorded.

Peaks were normalized to a base peak intensity of 100, and relative intensities were reported. All spectra were run at 70 eV ionizing energies, unless otherwise indicated.

b) MIKE spectra: To obtain the unimolecular MIKE spectrum of an ion, the magnet was tuned to pass only the desired ion, and the electric sector voltage was scanned. Using the relationship $E_1/E_2 = m_1/m_2$, the fragment daughter ions were identified, the peaks obtained were normalized to a base peak intensity of 100, and relative intensities were reported.

c) Kinetic energy release: To provide good energy resolution the ESA source and collector slits were narrowed until the main beam width was a minimum, i.e. 4-5 V at the base for the ZAB-2F. A slow scan of the ESA voltage, with the magnet tuned to transmit ions of the desired mass, allowed recording the metastable peaks. Values of T were calculated using:

$$T = \frac{m_1^2 \; Z \; eV}{16 \; m_2 \; m_3} \left(\frac{\Delta E}{E}\right)^2$$

for $m_1^+ \longrightarrow m_2^+ + m_3$

where

T: the kinetic energy release in eV units

m_1: mass of the precursor ion

m_2: mass of the daughter ion

m_3: mass of the neutral fragment

ΔE: width of the metastable peak at a selected height, in sector volt units

E: electric sector voltage at which normal ions are transmitted

The kinetic energy release was corrected for the natural width of the main beam, using the relationship (17):

$$W_h(corr) = (W_{hmb} - W_{hm}^*)^{1/2}$$

where

W_{hmb}: width of the main beam at a selected height

W_{hm}^*: width of the metastable peak at that height

A five parameter mathematical model devised by Holmes and Osborne, (32), was used to obtain the distribution of the kinetic energy release as a function of T, n(T).

d) Collision induced fragmentation spectra: The procedure was identical to that for MIKE spectra, except that helium gas at 6×10^{-7} mbar pressure was introduced to the 2nd FFR collision cell. Fragmentation peaks due to unimolecular decompositions in the 2nd FFR prior to the gas cell were also observed in the collision induced spectra; however, such peaks were not considered in the normalization process. Because there is no general agreement on how to report a CID spectra, a method of normalization was used in which each group of daughter ions was normalized to the most intense peak in that group, instead of the most intense peak in the spectrum.

The neutral products of ion fragmentatins were examined as follows (26). A positive voltage, approximately 800 V, was applied to the collision cell. All positively charged products could enter the gas cell and undergo collision induced dissociative ionization. The ionized neutral molecule, and its fragments, were then analysed by the electric sector as described above.

ii) Other Instruments:

Gas Chromatograph-Mass Spectrometer: A VG-Analytical 7070E mass spectrometer interfaced with a Dani 2800 gas-chromatograph and equipped with a mini computer data system was used for the analysis of the reaction products. This instrument was available at the Ottawa/Carlton Center for Mass Spectrometric Studies, Ottawa.

Proton NMR spectra were obtained using a Varian T-60 NMR spectrometer. The spectra of the labelled products were compared with those reported in the literature, when available, or with spectra of the unlabelled compounds under the same conditions, i.e. without the use of solvent or TMS.

Preliminary GC analysis was performed on a GOW-MAC series 750 gas chromatograph with a FID detector and a 6 foot by 0.125 inch, 3% O.V.-17 column.

Preparative gas chromatography was done using a PYE series 105 automatic GC equipped with a 99:1 column exit splitter, FID detector and 3% O.V.-17 column. The effluent of multiple 10 μl injections were collected in a capillary tube cooled in liquid nitrogen.

IV. RESULTS and DISCUSSION

A) Cyclohexenoxide and 5,6-dihydro-4-methyl-2H-pyran

Methyl loss is the only significant process observed in the MIKE spectra of the molecular ions of 5,6-dihydro-4-methyl-2H-pyran, 1, and cyclohexenoxide, 2. Both metastable peaks are extremely intense and there is no indication of instrumental insensitivity to other processes that might have been involved. To confirm that the C-4 substituent is the only site of the methyl radical loss from 1, the EI and unimolecular MIKE spectra of 5,6-dihydro-4,4,4-methyl-d_3-2H-pyran, 5, were examined. Negligible loss of CH_3, CH_2D or CD_2H were observed in the conventional spectrum, Fig. 7, and the unimolecular MIKE spectrum showed loss of CD_3 as the only detectable process in the second field free region. Therefore, the possibility of hydrogen scrambling prior to methyl radical loss could be ruled out and it may be concluded that C-4 substituent is the only source of methyl moiety eliminated.

Because of hydrogen transfer and loss of positional identity, Strong et al (3) were unable to define a unique pathway for methyl radical loss from 2 on the basis of conventional EI spectra and metastable peaks observed from

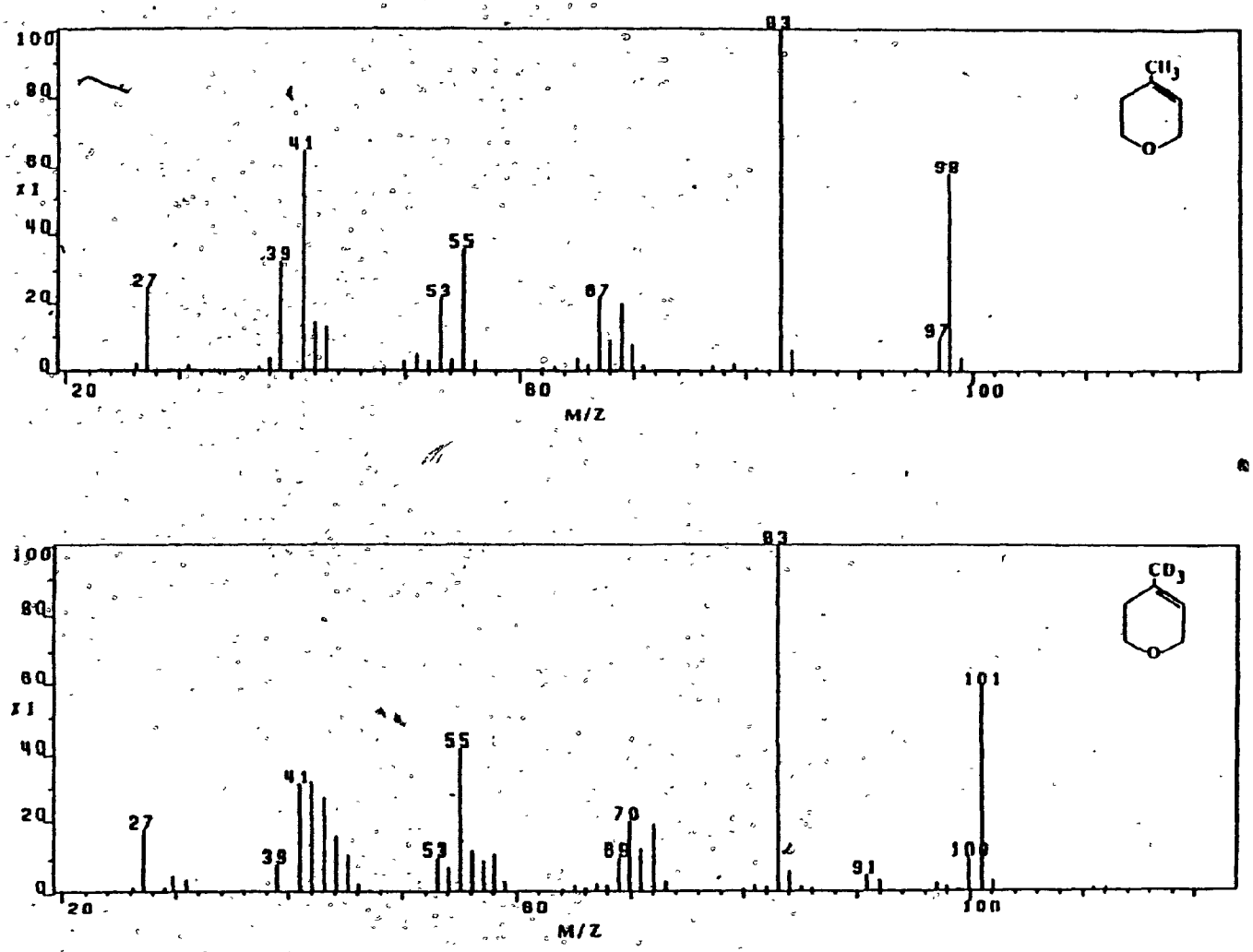

Fig.7. Mass Spectra of 1 and 5.

^2H labelled cyclohexeneoxides.

a) Thermochemical measurements:

Using energy selected electrons, (29), the ionization energy (IE) of 1 and 2 and the appearance energies (AE) of $[C_5H_7O]^+$ from these precursors were measured. Table 2 also shows the heat of formation of neutral molecules calculated from the group additivity contributions (33) and the heat of formation of daughter ions generated by methyl radical elimination.

Table 2, Thermochemical data corresponding to $[C_5H_7O]^+$ generated from 1 and 2.

	$\Delta H_f(M)$	$IE(M^{+\cdot})$	AE $[C_5H_7O]^+$	ΔH_f $[C_5H_7O]^+$
	(kJ/mol)	(eV)	(eV)	(kJ/mol)
5,6-dihydro-4-methyl-2H-pyran	-133	8.88	9.62	649
cyclohexen-oxide	-125	9.82	9.90	682

Because the AE value obtained for $[C_5H_7O]^+$ from 2 is very close to the IE of 2, the heat of formation of $[C_5H_7O]^+$ must be considered as an upper bound (IE limited). In our studies generally, an average AE-IE of ca. 0.3 eV was observed and hence a value in the vicinity of 653 kJ mol^{-1} may be more representative of the heat of formation of $[C_5H_7O]^+$ generated from 2.

ii) Metastable Peak Shape Analysis:

The methyl loss processes from the molecular ions of 1 and 2 in the second field free region gives rise to a non-composite and Gaussian-like metastable peak. Table 3 gives the T values obtained for this process.

Table 3, $T_{0.5}$ values for the $[M^{+\cdot}-CH_3^{\cdot}]$ process from 1 and 2.

	$T_{.5}$ (kJ/mol)	<T> (kJ/mol)	n
5,6-dihydro-4-methyl-2H-pyran	1.6	4.6	1.68
cyclohexen-oxide	2.5	7.5	1.63

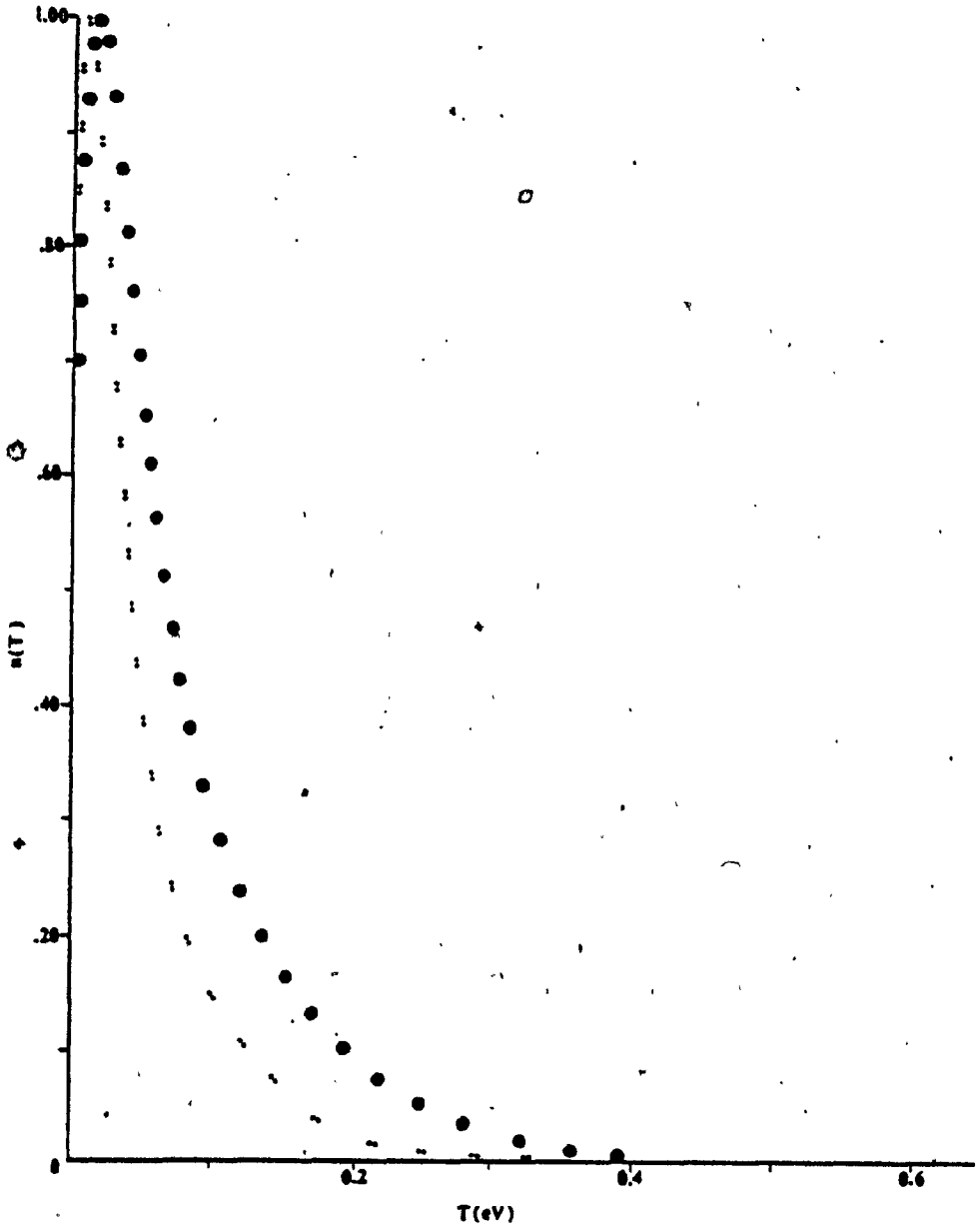

Fig.8. n(T) vs. T for $[M^{+\cdot} - CH_3^{\cdot}]$

•, cyclohexenoxide

–, 5,6-dihydro-4-methyl-2H-pyran

Note that reported $T_{0.5}$ values differ only by less than 1 kJ/mol. The n(T) curves show a high degree of sensitivity to the presence of a second component in the metastable peak (34). Fig.8 shows the distribution of kinetic energy release, n(T) vs. T curves, calculated by the method of Holmes and Osborne (32). For loss of methyl radical from 1 and 2 in the second field free region there is no indication of a second reaction channel in either case.

iii) Collision Induced Dissociation Spectra

The CID/MIKE spectra of source generated m/z 83 ions from 1 and 2 and 5,6-dihydro-4-methoxy-2H-pyran, 6, are shown in Table 4. Spectra obtained from 1 and 6 are quite identical. The least squares plot of peak intensities suggested by Lehman et al, (35), gives the correlation coefficient of r=0.991 for the spectra of 1 and 6. Values of r equal to or greater than 0.95 are considered as indicative of very similar spectra. For the spectra obtained from 1 and 2 the value of r=0.964, supporting the possibility of identical daughter ion structures (or mixture of structures), Fig.9. Because of the method of normalization, small variations in the relative intensities are magnified,

Table 4, Collision Induced Dissociation Spectra of $[C_5H_7O]^+$ ions from 1, 2 and 6.

	Source of $[C_5H_7O]^+$								
m/z	1a	2a	6a	1b	2b	6b	1c	2c	6c
	Relative Intensity								
26	24	24	25	23	26	26	26	27	27
27	100	100	100	100	100	100	100	100	100
28	20	20	18	19	22	22	20	24	24
29	68	73	68	70	75	74	66	74	68
31	5	6	4	6	4	5	3	3	4
37	16	16	22	16	18	17	19	20	18
38	32	30	32	31	31	31	35	39	37
39	100	100	100	100	100	100	100	100	100
41	7	7	8	7	7	8	10	10	10
42	7	6	7	7	6	6	5	4	5
43	31	21	31	33	19	33	20	11	24
50	39	46	41	36	46	37	34	48	33
51	46	53	49	44	52	47	42	52	43
53	100	100	100	100	100	100	100	100	100
54	26	47	29	28	48	35	23	55	26
55*	258	252	226	267	243	261	83	136	100
81	100	100	100	100	100	100	66	53	76
82	69	92	85	60	82	72	100	100	100

1a,2a,6a: source ions at 8 kV; 1b,2b: source ions at 7 kV; 6b: source ions at 6 kV; 1c,2c,6c: metastably generated in the first field free region.

*due to unimolecular contribution CID abundance of m/z 55 not included in normalizations.

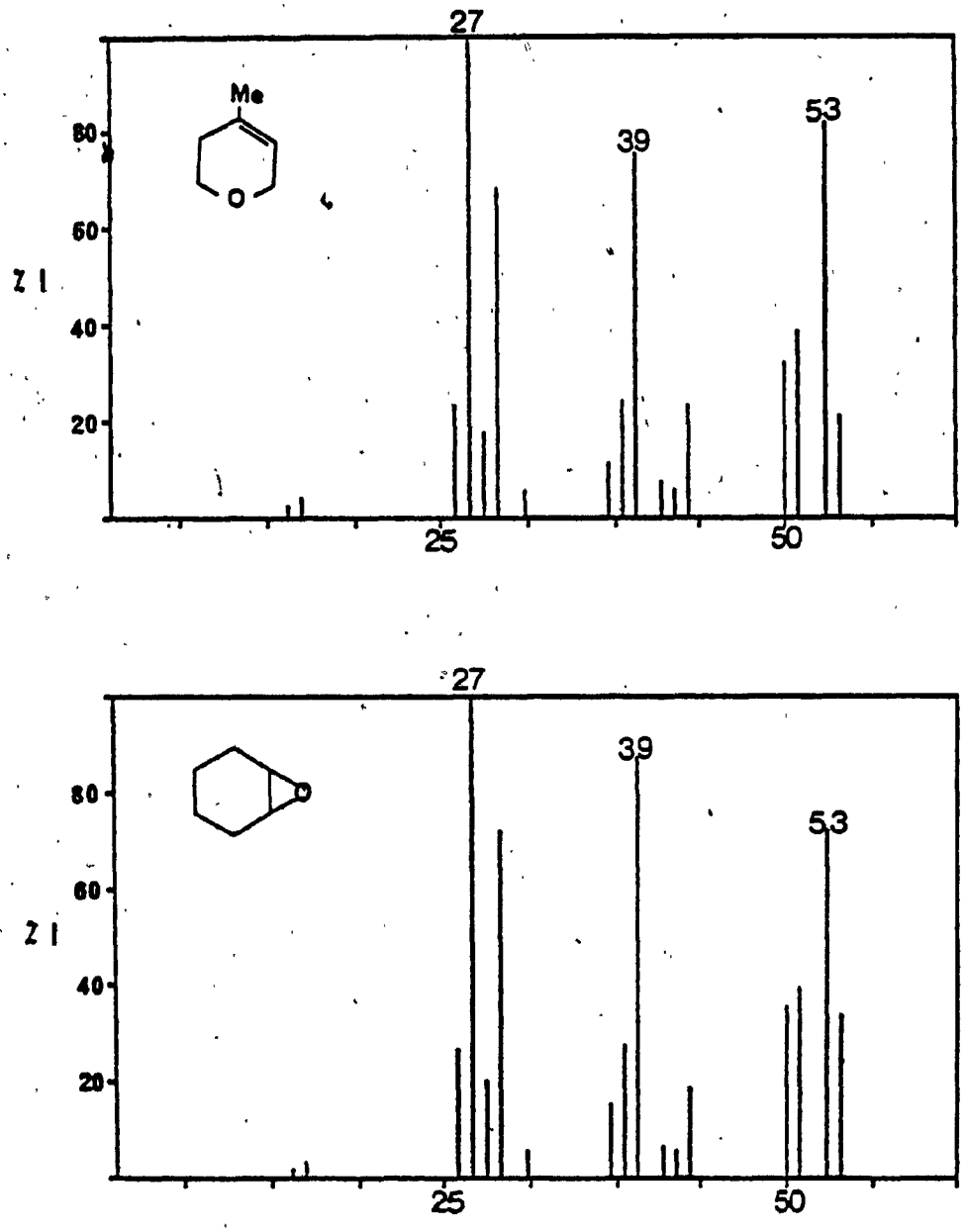

Fig.9. Partial CID spectra of source m/z 83 from 1 and 2.

particularly for peaks at m/z 82, 81 and 54. Peak intensities at m/z 81 and 82 have small contributions from unimolecular processes which are not corrected for here. The peak at m/z 54 follows a very intense peak at m/z 55 which may degrade the resolution and the accuracy of the measurement.

The CID/MIKE spectra of metastably generated ions are comparable to those obtained from the source m/z 83 ions. Some differences are observed in the relative abundances of m/z 82 and 81, which can be explained in terms of time and energy required for isomerization. For source generated ions, isomerization may be considered complete, and the CID/MIKE spectra represent the most stable ion stucture. On the other hand, the metastably generated ions sampled by the collision induced dissociation process may not be in their most stable configuration, i.e. isomerization may not yet be completed.

The unimolecular MIKE spectra of source generated m/z 83 ions from 1, 2 and 6 are essentially identical and have only one peak at m/z 55, corresponding to loss of a mass 28 neutral. Metastable peaks for this process were analyzed under condition of good energy resolution. The composite nature of each peak is shown in Fig. 10. The magnitude of the kinetic energy release is very similar in each case, giving an average of $T_{0.5}$= 222± 10 meV and an average <T> value of 347± 5 meV.

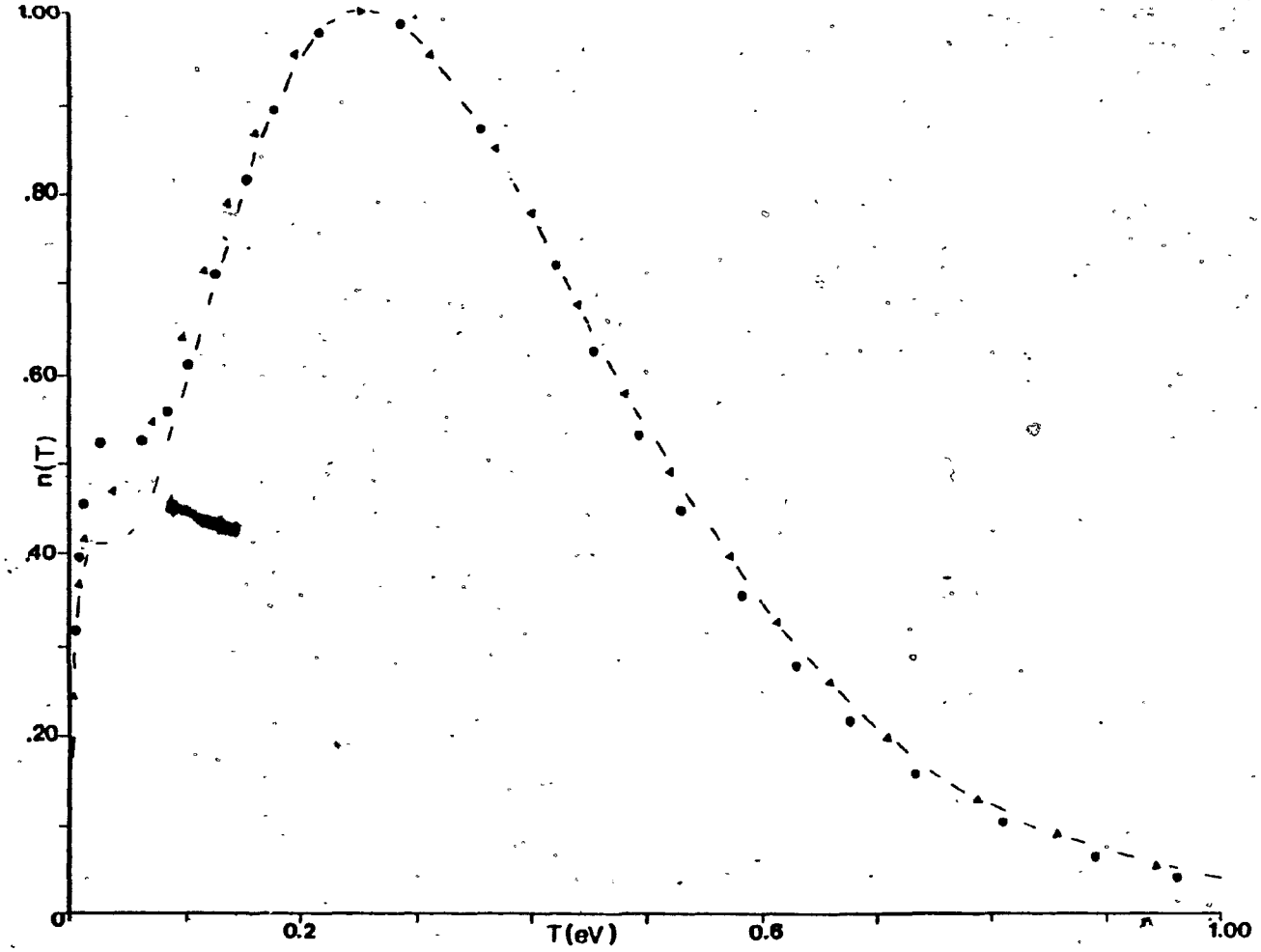

Fig.10. n(T) vs. T for [m/z 83 to 55]; —, cyclohexenoxide ●, 5,6-dihydro-4-methyl-2H-pyran; ▶, 5,6-dihydro-4-methoxy-2H-pyran.

Using the method suggested by Burgers et al, (26), for determination of the neutral products of ion fragmentations, only one peak at m/z 28 was observed for both 1 and 2, identified as loss of CO, as the following:

$$[C_6H_{10}O]^{+\cdot} \xrightarrow{-CH_3\cdot} [C_5H_7O]^{+} \xrightarrow{-CO} [C_4H_7]^{+}$$

This, in addition to the results presented above, confirms the hypothesis of a common daughter ion from the molecular ions of 1 and 2, both at threshold and 70 eV. The ion structure proposed is also in accordance with one of the mechanisms suggested by Strong et al, (3), as shown in the following scheme:

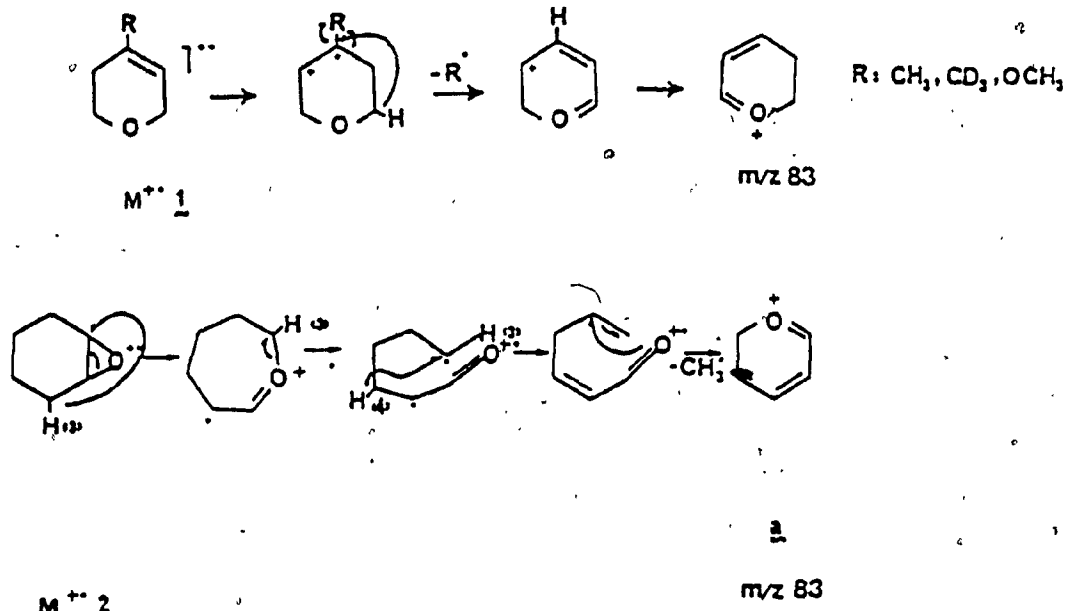

Scheme V.I

It should be noted here that the possibility of having more than one ion structure exists. Other structures, if present, would contribute to the minor differences observed in the CID/MIKE spectra. However, should a mixture of ion structures exist, the same mixture is generated from 1 and 2.

B) Mesityl Oxide, and Methyl-1-Methyl-Cyclopropyl Ketone

i) Metastable Peak Characteristics

Methyl radical loss is the only detectable process in the MIKE spectrum of the molecular ion of mesityl-oxide, 3. A narrow Gaussian-like second field free region metastable peak (T.5= 21 meV; <T>= 57 meV, n= 2.71) is associated with this fragmentation. Examination of the n(T) curves does not suggest the presence of a second reaction channel, Fig.11. Hydrogen atom exchange prior to or during methyl radical elimination is possible. However, based on the results of Zwinselman et al., (4), for the time scale appropriate to the second field free region the resulting ion would still have structure d, as shown below:

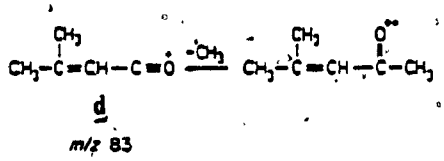

d
m/z 83

Scheme V.II

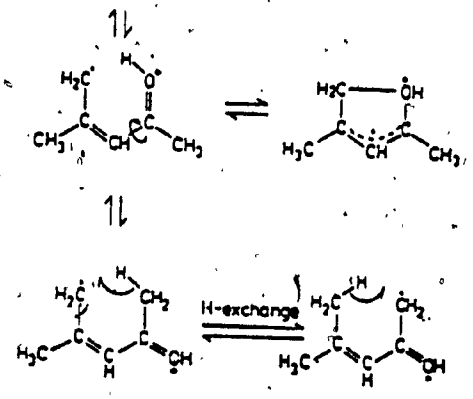

The MIKE spectrum of the molecular ion of methyl-1-methyl-cyclopropyl ketone is:

m/z 98 to	97	83	80	70	69	56	43
R.I.(%)	62	36	5	3	4	2	100

As is obvious, methyl radical loss is a major fragmentation route. The associated second field-free region metastable peak is a composite, with a measured $T_{0.5}$ of 45 meV, Fig.12-a. Deuterium labelling of the terminal methyl group, 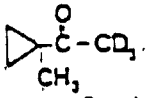 ,7 , results in essentially complete deconvolution of the composite peak into a narrow component ($T_{0.5}$=20 meV) for $[M^{+}\cdot - CD_3\cdot]$ and a broad peak for $[M^{+}\cdot - CH_3\cdot]$, Fig.12b. Loss of water from the molecular ion of methyl-1-methyl-cyclopropyl ketone, 4, is about 15% of the methyl radical loss. Thus the small second component seen in the n(T) distribution for $CD_3\cdot$ loss, Fig.13, may be attributed to the loss of water. This does not introduce a significant error in the $T_{0.5}$ value, but is reflected in the <T> value of 76 meV.

ii) Heats of Formation of Threshold Configurations:

Ionization energies (IE) of 3 and 4, and the appearance energies (AE) of $[M^{+}\cdot - CH_3\cdot]$ from these precursors were measured, using monoenergetic electrons, as described by Lossing et al, (29). Heats of formation

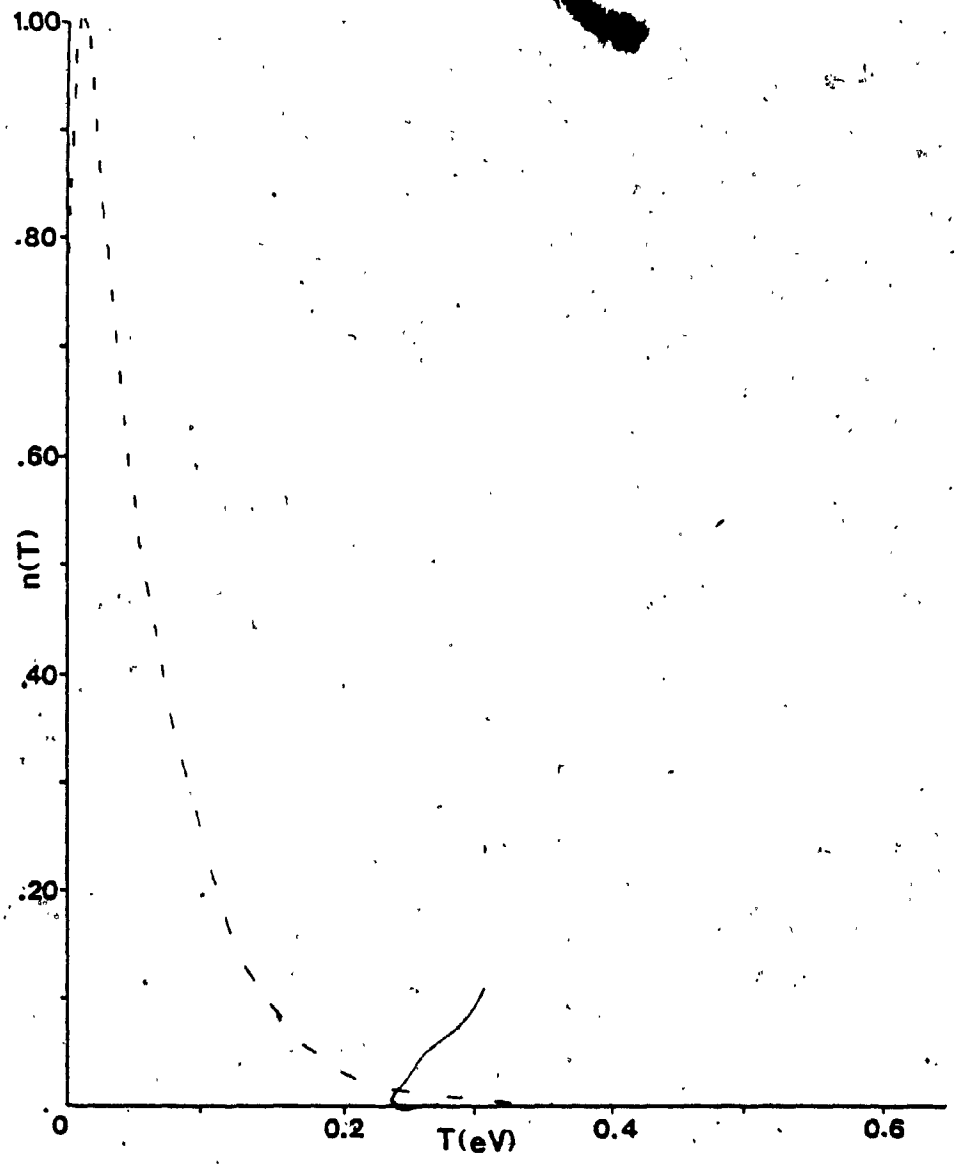

Fig.11. n(T) vs. T for $[M^{+\cdot} - CH_3^{\cdot}]$ from mesityl oxide.

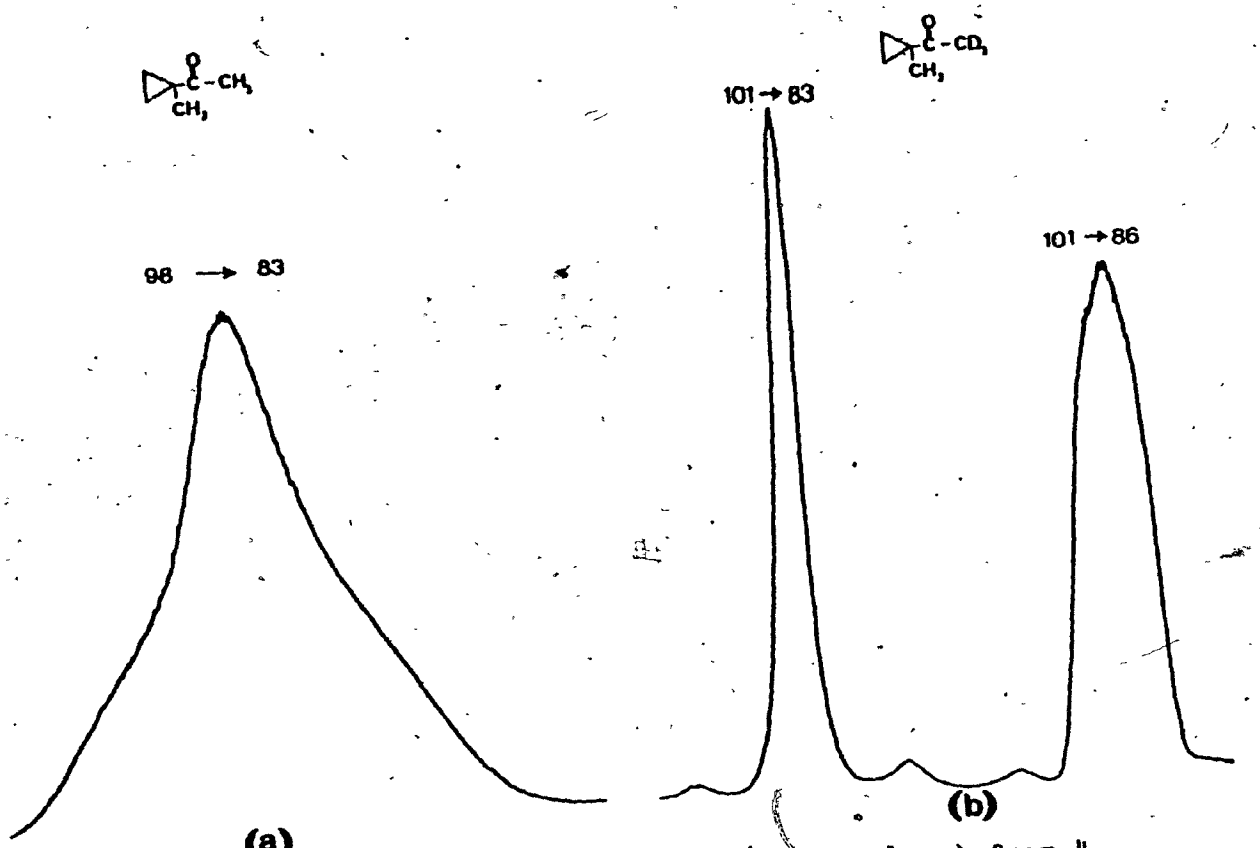

Fig.12. Metastable peak shape for $[M^{+\cdot} - CH_3^{\cdot}]$, a) from 4 b) from 7.

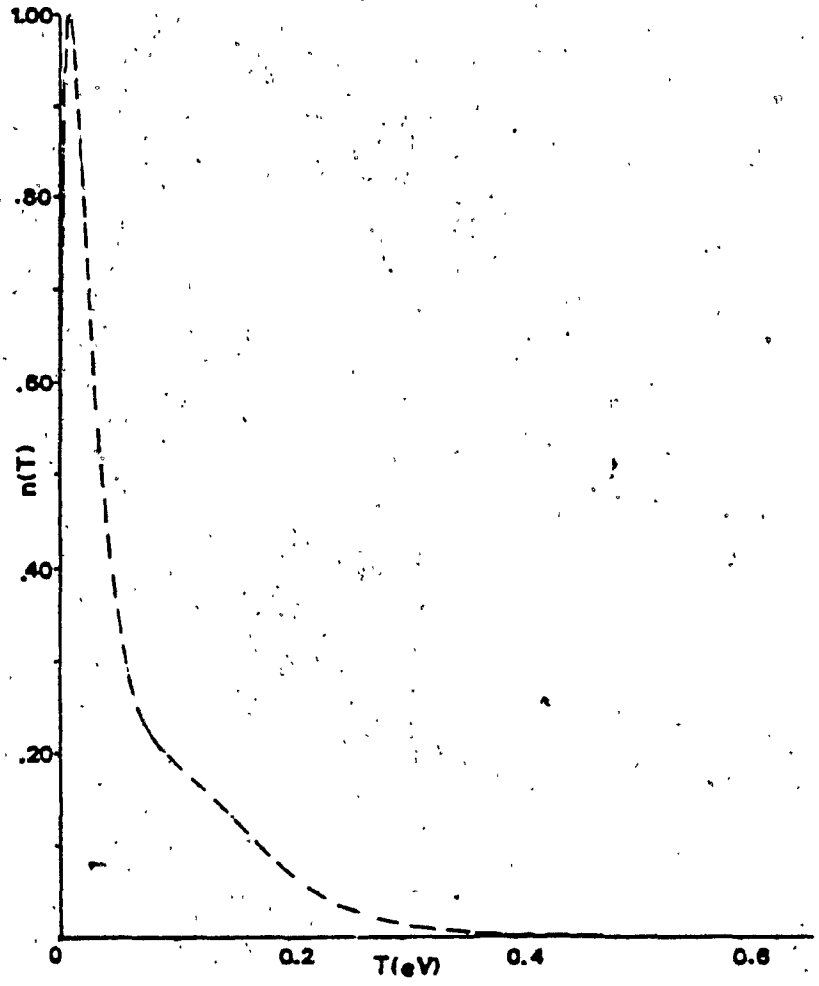

Fig.13. n(T) vs. T for $[M^{+\cdot} - CD_3^{\cdot}]$ from 7.

of the neutral molecules were calculated using the Benson additivity method, (33). The results obtained are summarised in table 5.

Table 5, Thermochemical data corresponding to methyl loss from 3 and 4.

	$\Delta H_f(M)$ (kJ/mol)	IE (eV)	AE (eV)	$\Delta H_f[C_5H_7O^+]$ (kJ/mol)
Mesityl-oxide	89	9.10	9.48	577
Methyl-1-Methyl-Cyclopropyl Ketone	-136	9.24	9.88	669

The different values obtained for $\Delta H_f[C_5H_7O^+]$ from 3 and 4 can be attributed to generation of daughter ions of different threshold configuration. Metastable AE measurements for loss of 15 u and 18u from 7 show that, as might be expected, the threshold loss of methyl radical from 4 does not involve the α-CH_3 group, i.e. simple cleavage, and it is assumed that the C(1) substituent is the one being eliminated, although additional labelling experiments are needed to establish this point. According to Quasi-Equilibrium Theory, rearrangement reactions require less activation energy and are more dominant at lower energy levels than simple cleavage type reactions.

which are seen more often at higher internal energy levels (15). As the loss of 15 u may involve rearrangement, it takes place at lower ionization energy than the simple cleavage loss of 18 u.

The proposed formation threshold configuration of d from mesityl oxide was further ascertained by application of a scheme suggested by Holmes and Lossing for estimating the heats of formation of gas-phase organic ions (36, 37). These authors showed that successive methyl substitutions at the charge bearing site results in a straight line plot for ΔH_f(ion) vs. log (no. of atoms). The first ion in the series of interest, generated by loss of CH_3 from ionized methyl-vinyl ketone, (38), could have either canonical structures shown below:

$$CH_2{=}HC{-}\overset{+}{C}{=}O \longleftrightarrow H_2\overset{+}{C}{-}HC{=}C{=}O$$

k

Loss of a hydrogen atom from crotonaldehyde gives rise to the second ion in this series, (39), and ion d can be seen as a doubly CH_3 substituted ion k. The line drawn through these points lies almost parallel to corresponding plots for other series of methyl substitution at charge bearing sites. Fig.14, shows that the least squares line C, passing through d, k and l, is approximately parallel to lines A and B chosen from (37). The data used are given in Table 6. The straight line plot confirms d as the proposed structure of the ion generated by CH_3· loss from 3.

Table 6, Data used in plot of ΔH_f[ion] vs. log n, (Fig.14)

Line	Structure	n	ΔH_f[ion] (kJ/mol)	log n	ref.
	CH_2O	4	942	0.602	37
A	CH_3CHO	7	818	0.845	37
	$(CH_3)_2CO$	10	720	1.000	37
	CH_2OH	5	703	0.699	37
B	CH_3CHOH	8	582	0.903	37
	$(CH_3)_2OH$	11	502	1.040	37
	$CH_2=CH-C^+=O$	7	749	0.845	38
C	$CH_3CH=CH-C^+=O$	10	690	1.000	16
	$(CH_3)_2C=CHC^+=O$	13	577	1.114	this work

Least squares line equations:

C	slope= -624.371	Intercept=	1287.84
B	-589.728		1115.02
A	-553.582		1278.21

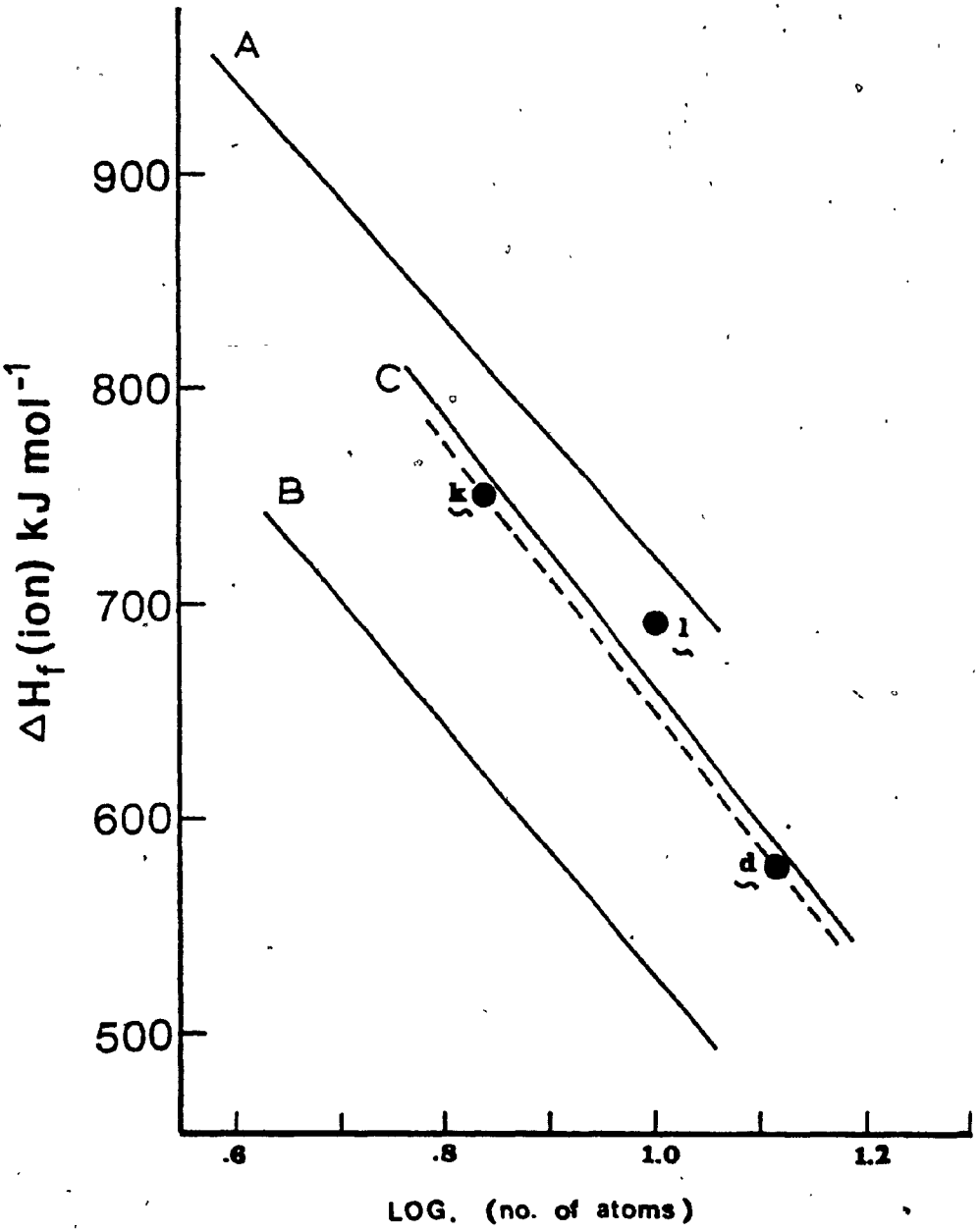

Fig.14. ΔH_f[ion] for successive substitution of $-CH_3$ vs. log (no. atoms).

The AE value used to obtain the heat of formation of ion 1 was measured using a conventional electron impact source and the semi-logarithmic method. This approach is known to yield relatively inaccurate AE values (16). The distance between point 1 and the line C may be taken as a correction term for the heat of formation of 1.

Therefore, even though α-cleavage seems to be a secondary process, relative to rearrangement, at formation threshold energies, because of resonance stabilization in the ion d there is no competition between simple cleavage and rearrangement in the generation of $[C_5H_7O^+]$ from mesityl oxide. Only ion d resulting from α-cleavage is seen at the formation threshold.

iii) CID/MIKE Spectra:

The CID/MIKE spectra of source generated m/z 83 ions from 3,4 and 7 are given in Table 7. The very intense peak observed at m/z 55 contains a contribution

from the unimolecular (MIKE) decomposition in all three cases. Therefore, the intensity of the m/z 55 peak was not taken into consideration when measuring the CA spectra. The CID/MIKE spectrum of m/z 86 generated from 7 has a significant peak at m/z 46, indicating that the corresponding m/z 43 from 4 can be rationalized as:

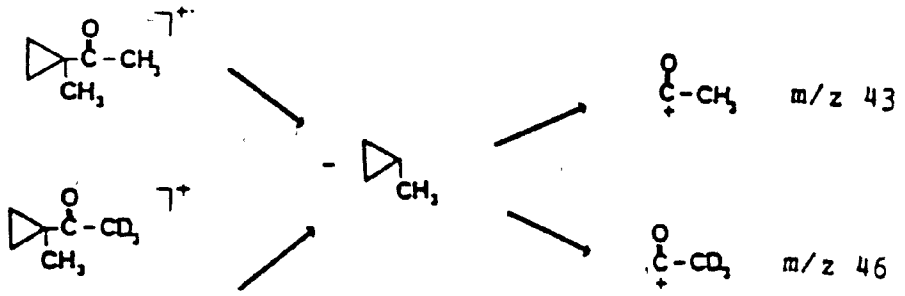

The presence of a small amount of unlabelled material is assumed by the small m/z 43 peak in the CID/MIKE spectrum of 7. The relative abundances of peaks at m/z 82, 81 and 54 from 3 are significantly lower than the ones from 3 and 7. These peaks may be indicative of characteristic differences in the ions of m/z 83 from these precursors. Perhaps the generation of a resonance stabilized ion d (from 3) decreases the availabilty of hydrogens to be lost following collisional activation, but this process has not been studied in any detail in this work.

It was proven by studying the collision induced dissociation spectra of the neutral fragment ions that the process [m/z 83 to 55] involves the loss of CO in the case of 3 and 7.

Table 7, Collision induced dissociation spectra of $[C_5H_7O]^+$ ions from 3, 4 and 7.

m/z	Source of Ion 3	4	7
	Relative Intensity		
26	3	5	4
26	16	27	25
27	100	100	100
28	16	20	19
29	79	61	64
37	17	23	16
38	32	34	28
39	100	100	100
40	19	17	19
41	11	9	10
42	7	8	5
43	4	38	13
50	65	55	52
51	66	52	54
53	100	100	98
54	46	84	100
81	21	75	67
82	100	100	100

$[C_5H_7O]^+$ source ions at 8 kV.

Due to MI contributions, peak intensities of m/z 55 are not reported.

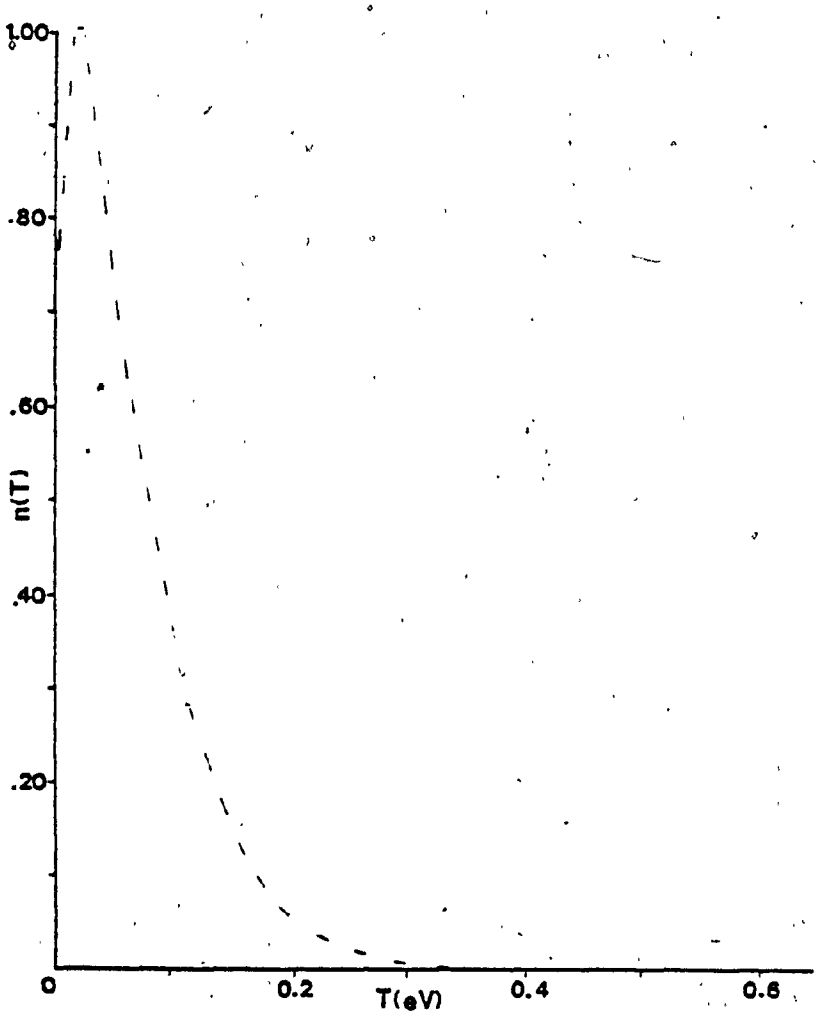

Fig.15. n(T) vs. T for [m/z 83 to 55] from mesityl oxide.

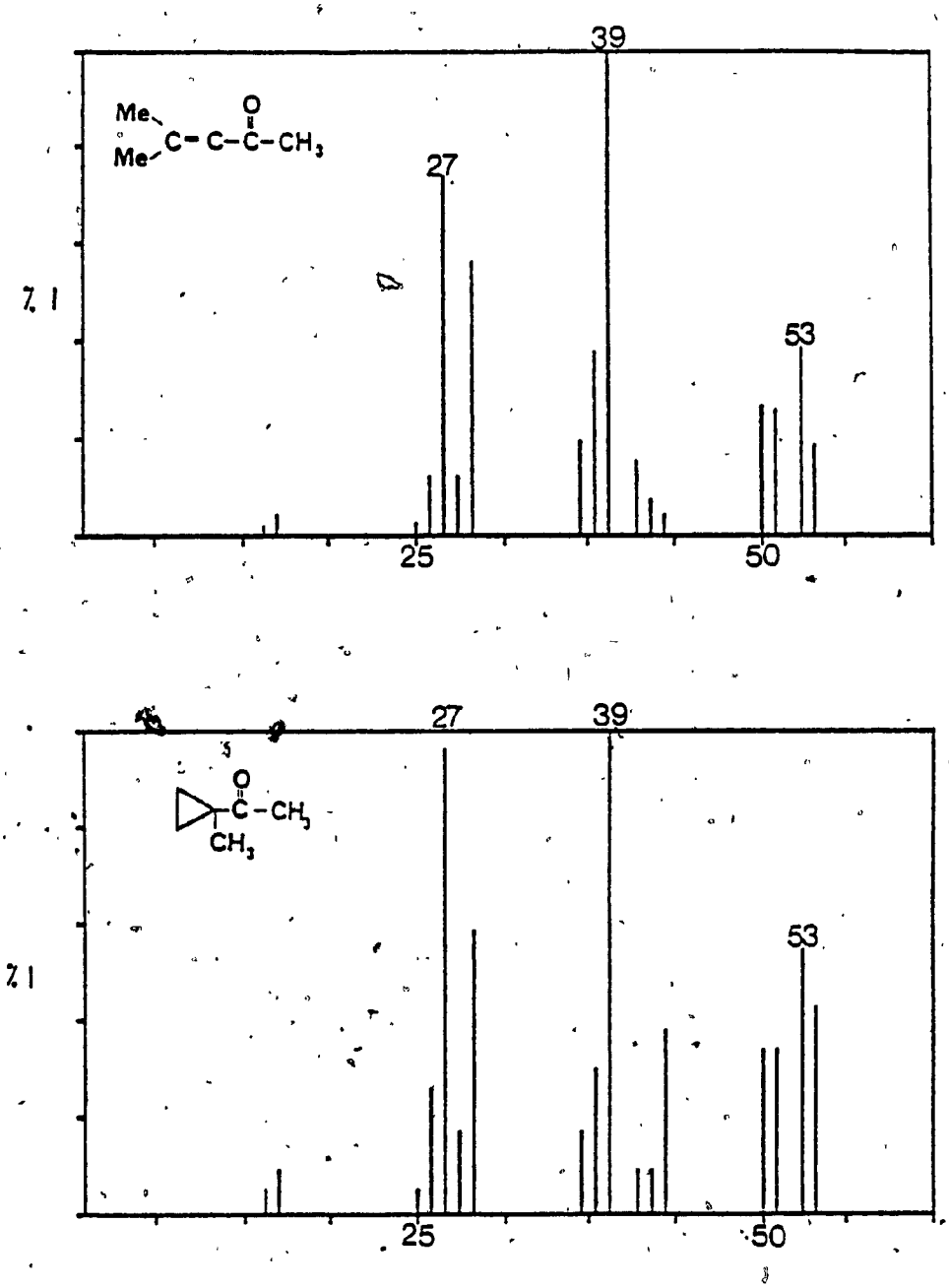

Fig.16. Partial CID spectra of source m/z 83 from 3 and 4.

Table 8, Collisional induced dissociation spectra of $[C_4H_7]^+$ ions from 3, 4 and 7.

	Source of Ion				
	3a	4a	7a	3b	7b
m/z	Relative Intensity				
25	3	4	3	2	3
26	19	18	18	19	20
27	100	100	100	86	91
28	16	16	16	9	11
29	73	75	76	100	100
37	12	12	13	10	11
38	20	22	23	16	17
39	100	100	100	100	100
49	9	11	12	7	9
50	54	59	54	33	37
51	58	63	55	31	35
52	13	15	15	6	8
53	100	100	88	100	100
54	30	100	100	8	18

3a, 4a, and 7a: metastably generated from m/z 83 in the first field free region, 3b and 7b: source ions at 8 kV.

In the metastable time frame this process is associated with (in the case of 3) a non-composite, Gaussian-type peak (T.5= 25 meV, <T>=68 meV) as shown in Fig.16. For 7 the corresponding metastable peak was also narrow (T.5= 26 meV), but because of impurities in the precursor m/z 83 ion the value of <T>= 125 meV, cannot be taken as being reliable. Other compounds studied- even some ketones- exhibited a much larger kinetic energy release for this process. Bowen et al, (40), studying the loss of Br· from five isomeric C_4H_7Br, reported that 1- and 2- methallyl-bromide molecular ions had a significantly small average kinetic energy release (0.4 kJ mol^{-1}).

Of the $[C_4H_7]^+$ ions studied by Lossing, (41), the heat of formation of the methyl allyl cation was reported to be the lowest (853±13 kJ/mol) with ΔH_f for the 2-methyl allyl ion being slightly higher (883±21 kJ/mol). The generation of 2-methyl allyl cation from mesityl oxide is expected, as following:

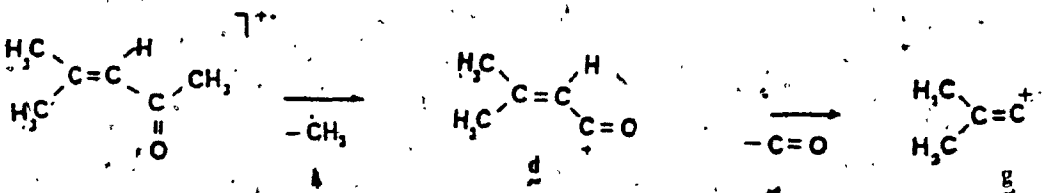

Scheme VIII

The generation of methyl allyl cation from methyl-1-methyl cyclopropyl ketone could follow the path shown here:

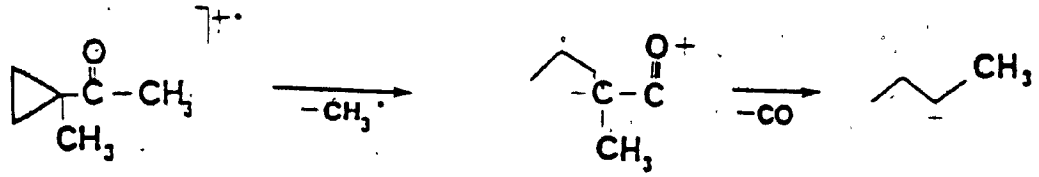

e f

Scheme V.IV

This scheme is in agreement with the one proposed by Schwarz et al., (7). Whether the cyclopropyl ring remains intact in the m/z 83 ion is questionable. However, if the ring had not opened, due to rearrangement, one would expect to observe a larger release of kinetic energy for m/z 83 to 55.

The CID/MIKE spectra of metastably generated m/z 55 from m/z 83 of 3 and 7 are given in Table 7. Except for the relative intensities of m/z 54 peaks, the spectra are similar. The minor differences observed may be due to isomeric structural differences. For source generated m/z 55 from 3 and 7 the CID/MIKE spectra are again quite similar. However, it should be taken into consideration

that the source m/z 55 ions may have a different configuration than the metastably generated entity. It should also be mentioned that, in a number of cases, collisional activation spectra fail to distinguish structural differences due to a lower energy barrier for isomerization than for fragmentaion. This is particularly true for hydrocarbon ions (42).

V. Conclusions and Suggestions for Further Studies

A)

On the basis of thermochemical data, metastable peak shape analysis and collision induced dissociation spectra it is concluded that the loss of methyl radical from the molecular ions of cyclohexenoxide and 5,6-dihydro-4-methyl-2H-pyran generates a common daughter ion, both at threshold and 70 eV. Ion c is most likely the structure of this daughter ion. Should a mixture of structures exist, ion c would be a major component of such mixture.

In the mechanism proposed by Strong et al, (3), the molecular ion of tetrahydroxepin is the intermediate ion in the process of methyl radical loss from cyclohexenoxide. There is no information available on the mass spectral behavior of tetrahydroxepin. Attempts have been made to prepare this compound and to study its fragmentation pathways, yet refinements in the synthetic procedure are required.

Because of hydrogen atom scrambling, site specific ^{13}C labelling of cyclohexenoxide is necessary to identify the methyl radical being eliminated.

CID/MIKE spectra of metastably generated m/z 55 from m/z 83 would also confirm the existence of a common daughter ion structure and provide information with regards to the $[C_4H_7]^+$ ion structure.

B)

Experimental results indicate the possibility of generating isomeric methyl-allyl ions from $[C_5H_7O]^+$ daughter ions of mesityl-oxide and methyl-1-methyl-cyclopropyl ketone. At present, evidence supporting the existence of a common $[C_5H_7O]^+$ from 3 and 4 is lacking.

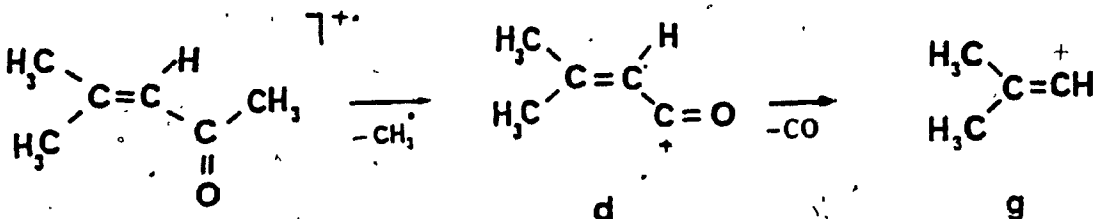

d g

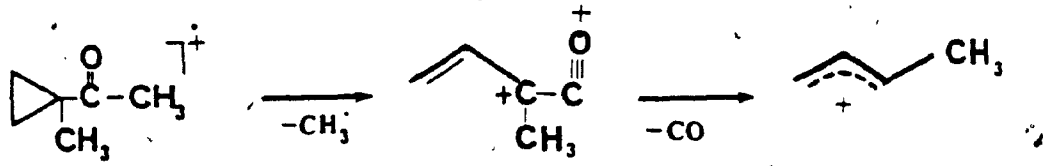

e f

As it can be seen from the above, it is postulated that the cyclopropyl ring is opened, at least, prior to the CO loss. Experiments finalizing the state of the cyclopropyl ring would be of great importance in confirming the structure of $[C_5H_7O]^+$ and $[C_4H_7]^+$ ions generated from 4 and 7.

The application of the plot of ΔH_f[ion] vs. log no. atom could be further extended to the estimation of the heat of formation of ion 9.

Also, since peak of m/z 55 in the spectra of 3 and 4 could be originated at least from two different sources, i.e. from [m/z 98 to 55] and/or from [m/z 83 to 55], the CID/MIKE spectra of m/z 55 is not pure and metastably generated m/z 55 ions should be looked at instead. In observing metastably generated m/z 55 from m/z 83 ions of 4 difficulties were encountered. The use of a triple sector analyzer in such instances is recommended.

Appendix:

i) Mass spectrum of 5,6-dihydro-4-CD_3-2H-pyran

m/z	R.I.(%)
27	17
41	31
42	31
43	26
44	15
53	10
55	41
56	11
58	11
69	10
70	19
72	19
83	100
100	10
101	58

ii) Mass spectrum of CD_3-1-methyl-cyclopropyl ketone

m/z	R.I.(%)
27	27
29	24
39	31
43	46
44	76
45	69
46	45
53	15
55	100
83	24
98	19
99	29
100	24
101	13

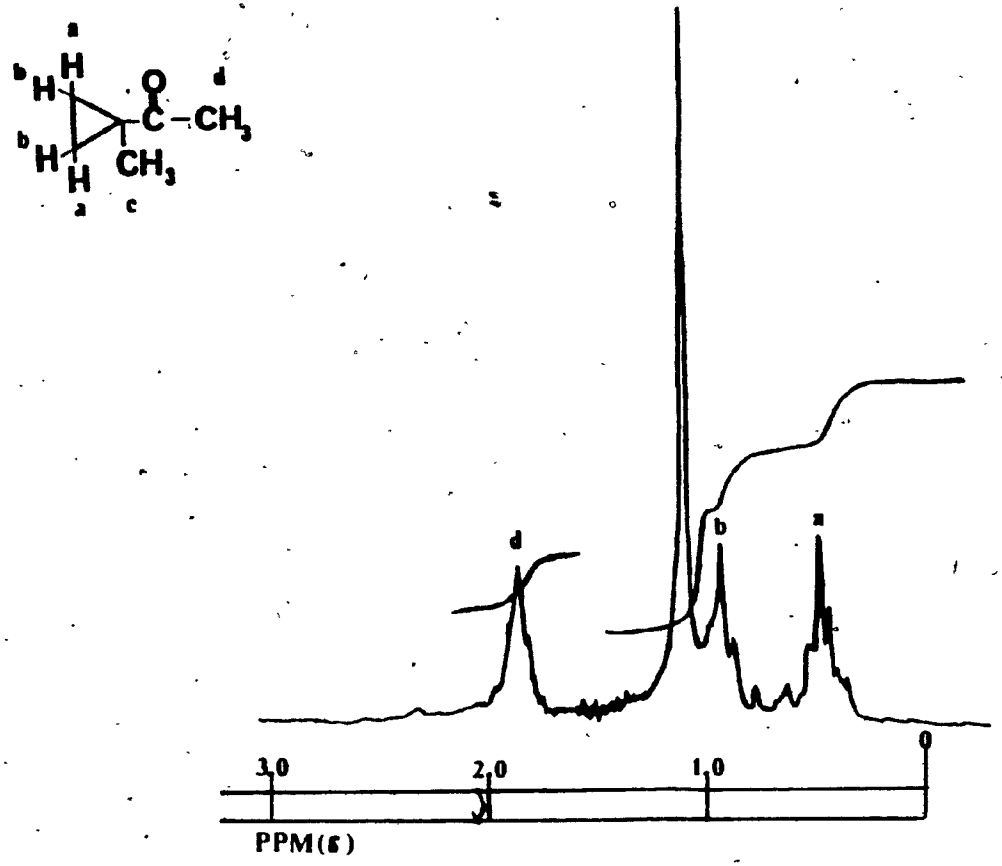

iii) NMR spectrum of CD_3-1-methyl-cyclopropyl ketone

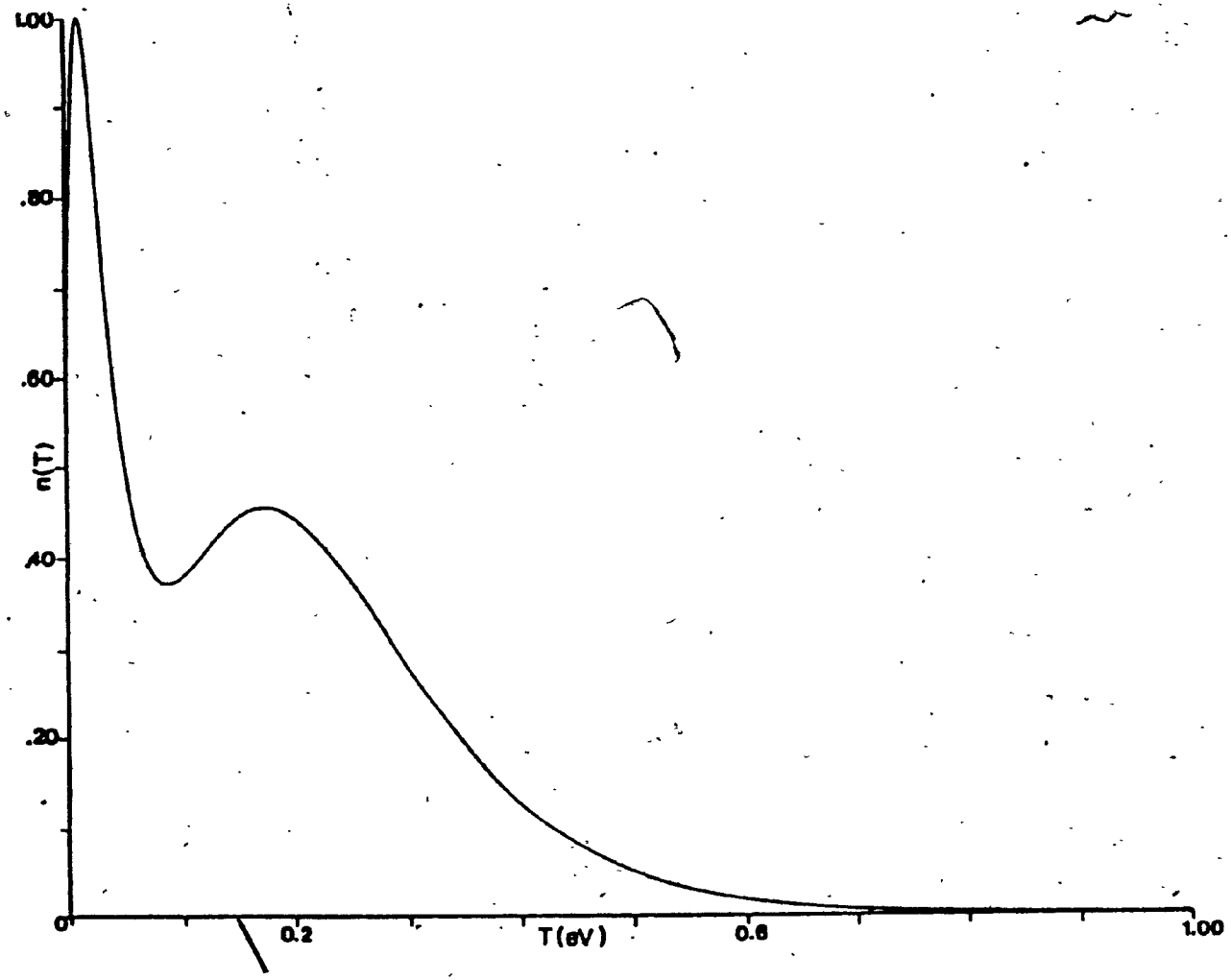

iv) n(T) vs. T for $[M^{+\cdot} - CH_3^{\cdot}]$ from methyl-1-methyl cyclopropyl ketone

REFERENCES:

1) N.S.Vul'fson, G.M.Zolotareva, V.n.Bockkarev, B.V.Unkovskii, V.B.Mochaiu, Z.I.Smolina and A.N.Vul'fson, IZZ. Akad. Nauk SSSR, Ser. Khim. 1125 (1970).

2) E.G.Galkin, E.M.Vyrypaev, N.A.Romanov, E.A.Kantor, A.M. Syrkim and D.L.Rakhmankulov, Zh. Prikl. Khim. (Leningrad), 55, 960 (1982).

3) K.M.Strong, P.Brown and C.Djerassi, Org. Mass Spectrom., 2, 1201 (1969).

4) J.J.Zwinselman, N.N.Nibbering, B.Ciommer and H.Schwarz, Current Topics in Mass Spectrometry and Chemical Kinetics, Eds. J.H.Beynon and M.L.McGlashan, Heyden and Son, London (1982).

5) B.Ciommer, W.Zummack, H.Schwarz and N.N.Nibbering, Org. Mass Spectrom., 17, 152 (1982).

6) F.Borchers, K.Levsen, H.Schwarz, C.Wesdemiotis and R.Wolfschutz, J. Am. Chem. Soc. 99, 1716 (1977).

7) H.Schwarz, C.Wesdemiotis, K.Levsen, H.Heinebach and W. Wagner, Org. Mass Spectrom., 14, 244 (1979).

8) R.P.Morgan, J.H.Beynon, R.H.Bateman and B.N.Green, Int. J. Mass Spectrom. Ion Phys., 28, 171 (1978).

9) J.H.Beynon, R.M.Capriolli and T.Ast, Org. Mass Spectrom., 5, 229 (1971).

10) R.G.Cooks, J.H.Beynon, R.M.Capriolli and G.R.Lester, Meta-

stable Ions, Chapter I, Elsevier, Amsterdam (1973).

11) C.J.Porter, J.H.Beynon and T.Ast, Org. Mass Spectrom., 16, 101 (1981).

12) J.H.Beynon, F.M.Harris, B.N.Green and R.H.Bateman, Org. Mass Spectrom., 17, 55 (1982).

13) K.Levsen, Fundamental Aspects of Organic Mass Spectrometry, Chapter V, Verlag Chemie, Weinheim (1978).

14) P.Longevialle, Principes de la Spectrometrie de Masse des Substances Organique, Masson, Paris (1980).

15) J.L.Holmes and F.P.Lossing, Current Topics in Mass Spectrometry and Chemical Kinetics, Eds. J.H.Beynon and M.L.McGlashan, Heyden and Son, London, (1982).

16) H.M.Rosenstock, K.Draxl, B.W.Steiner and J.T.Herron, J.Phys. Chem., Ref. Data 6, Suppl.1, 6 (1977).

17) J.L.Holmes and J.K.Terlouw, Org. Mass Spectrom., 15, 383 (1980).

18) A.N.H.Yeo and D.H.Williams, J. Am. Chem. Soc., 93, 395 (1971).

19) C.Lifshitz, P.Gotchiguian and R. Roller, Chem. Phys. Lett., 95, 106 (1983).

20) R.G.Cooks, Collision Spectroscopy, Chapter VII, Ed. R.G. Cooks, Plenum Press, New York (1978).

21) M.S.Kim and F.W.McLafferty, J. Am. Chem. Soc. 100, 3279 (1978).

22) F.W.McLafferty, Tandem Mass Spectrometry, John Wiley and

Sons, New York (1983).

23) K.Levsen and H.Schwarz, Angew Chem. Int. Ed. Engl. 15, 509 (1976).

24) C.J.Porter and J.H.Beynon, Int. J. Mass Spectrom. Ion Phys., 28, 321 (1978).

25) P.C.Burgers, J.L.Holmes and J.H.Beynon, Org. Mass Spectrom., 16, 62 (1981).

26) P.C.Burgers, J.L.Holmes, A.A.Mommers and J.K.Terlouw, Chem. Phys. Lett. 12, 1 (1983).

27) P.C.Burgers, J.L.Holmes, A.A.Mommers, J.E. Szulejko and J.K.Terlouw, Org. Mass Spectrom. 19, 442 (1984).

28) S.Cabiddu, A.Maccioni and M.Secci, Gazz. Chim. Ital., 100, 939 (1970).

29) K.Meda, G.P.Semeluk and F.P.Lossing, Int. J. Mass Spectrom., Ion Phys., 1, 395 (1968).

30) F.P.Lossing and J.C.Traeger, Int. J. Mass Spectrom., Ion Phys., 19, 9 (1976).

31) P.C.Burgers and J.L.Holmes, Org. Mass Spectrom., 17, 123 (1982).

32) J.L.Holmes and A.D.Osborne, Int. J. Mass Spectrom. Ion Phys., 23, 189 (1977).

33) S.W.Benson, F.R. Cruikshank, D.M.Golden, G.R.Haugen, H.E. O'Neal, A.S.Rogers, R.Shaw and R.Walsh, Chem. Rev., 69, 279 (1969).

34) J.L.Holmes and A.D.Osborne, Org. Mass Spectrom., 16, 236

(1981).

35) T.A.Lehman, M.M.Bursey and J.R.Hass, Org. Mass Spectrom., 18, 373 (1983).

36) J.L.Holmes, M.Fingas and F.P.Lossing, Can. J. Chem., 59, 80 (1981).

37) J.L.Holmes amd F.P.Lossing, Can. J. Chem., 60, 2365 (1982).

38) J.L.Holmes, J.K.Terlouw and P.C.Burgers, Org. Mass Spectrom., 15, 140 (1980).

39) H.H.Hommes and J.K.Terlouw, Org. Mass Spectrom., 14, 51 (1979).

40) R.D.Bowen, D.H.Williams, H.Schwarz and C.Wesdemiotis, J. Chem. Soc. Chem. Comm., 261 (1979).

41) F.P.Lossing, Can. J. Chem., 50, 3973 (1972).

42) D.L.Kemp and R.G.Cooks, Collision Spectroscopy, Chapter V, Ed. R.G.Cooks, Plenum Press, New York (1978).